Measurement and Compensation of Digital to Analog Converter Nonlinearity

By

Gregory A. Friel

B.S. University of Maine, 1998

A THESIS

Submitted in Partial Fulfillment of the

Requirements for the Degree of

Master of Science

(in Electrical Engineering)

The Graduate School

University of Maine

May, 2000

Advisory Committee:

Donald M. Hummels, Professor of Electrical and Computer Engineering, Advisor

Fred H. Irons, Castle Professor of Electrical and Computer Engineering

David E. Kotecki, Associate Professor of Electrical and Computer Engineering

LIBRARY RIGHTS STATEMENT

Measurement and Compensation of Digital to Analog Converter Nonlinearity

By Gregory A. Friel

Thesis Advisor: Dr. Donald M. Hummels

An Abstract of the Thesis Presented

in Partial Fulfillment of the Requirements for the

Degree of Master of Science

(in Electrical Engineering)

May, 2000

A novel method of finding digital to analog converters(DAC) input sequences to produce high-fidelity output waveforms is presented. Error produced by a non-ideal DAC is represented by its spectral components. Successive power spectrum measurements are used to solve for the unknown amplitude and phase of compensation signals applied to the DAC input. This iterative technique has produced waveforms that have a reduction in harmonic distortion. This iterative method of finding error can also be used to develop dynamic models of the error introduced by the DAC based on current and previous DAC input codes. These models can predict and correct errors produced from an arbitrary input sequence. An evaluation of this technique will be done using a 300 MSPS 12-bit DAC.

ACKNOWLEDGMENTS

This work has been supported in part by the DARPA Digital Receiver program under a contract administered by the Office of Naval Research Gr N66001-97-C-8617.

This work could not have been made possible without the support of my dog, Rafter.

TABLE OF CONTENTS

LIST OF FIGURES

CHAPTER 1

Introduction

1.1 Background

High speed digital to analog converters(DACs) are increasingly common components of systems requiring high quality analog signal synthesis. Communications applications such as direct intermediate frequency(IF) synthesis require broadband DACs exhibiting low intermodulation distortion. DACs are now common in high performance test and measurement equipment which require accurate waveform synthesis to excite external devices. Further, low distortion DACs are essential building blocks for many important analog to digital converter(ADC) architectures, and may also provide test waveforms for automatic calibration of ADCs or other measurement systems.

This thesis investigates the measurement and description of distortion which is introduced by high speed, high resolution DACs. A fundamental assumption in this presentation is that the DAC specifications exceed those of available ADCs. That is, it is not possible to directly sample and evaluate the DAC output waveform using an ADC at the same or higher speed. Methods must be developed which measure the critical distortion characteristics without requiring a broadband capture of the output waveform.

Two related procedures are developed. First, a calibration scheme is introduced which determines a DAC input sequence which is required to generate a particular high fidelity(low distortion) output waveform. This procedure is directly applicable to the use of DACs for generation of calibration waveforms for high-performance measurement systems. It has been successfully applied to the problem of fast calibration of ADC's for receiver applications[2, 3]. Second, DAC distortion is modeled so that the distortion associated with an arbitrary input sequence may be anticipated and compensated by modification of the sequence used to drive the DAC. This aspect of DAC distortion compensation is applicable for arbitrary waveform generation(e.g., direct IF synthesis) or for the use of linearized DACs for ADC architectures. This is a much more difficult problem, and is met with mixed results. Chapter 3 presents a previously proposed distortion model and describes a calibration procedure which is capable of solving for the required model parameters. Hardware implementation of the procedure has not shown the expected performance improvement, suggesting that the proposed model may not be appropriate for this tested DAC.

Previous work focused on developing a general error model for arbitrary waveforms[1, 4, 5]. This previous research developed a method of collecting data from the output of a DAC using an ADC at a reduced sample rate and extracting error information from data to create a model. The configuration of the calibration setup was quite elaborate and required careful synchronization of the ADC output and DAC input. The DAC calibration system itself required a long calibration process to determine timing between the DAC samples and the ADC samples. Also, all gains and phase shifts for the system were required in order to account for analog signal delays. This configuration provided a reduction in harmonic distortion of the DAC output but did not provide results that would be suitable for ADC calibration. It was not clear whether the failure of the technique was due to short-comings of the calibration system or the selection of an inappropriate DAC model.

1.2 Thesis Overview

This thesis introduces an alternate calibration technique which eliminates the need for coherence between the DAC input and the measurement system, thus greatly simplifing the calibration hardware and algorithms.

Chapter 2 discusses DAC calibration for waveform generation. Methods of determining error for a given waveform are discussed and results of compensation for a simulated and experimental DAC are presented.

Chapter 3 presents theory to generalize the error of a DAC using the error estimate provided by the method in Chapter 2. A least-squares method determines coefficients for Gaussian basis functions. Simulation and experimental results are included.

Chapter 4 discusses compensation results and provides insight to the shortcomings of this technique. Possible causes of distortion are examined and confirmed by simulation.

Chapter 5 draws further conclusions for this research and suggests further research that might be necessary.

CHAPTER 2

DAC Calibration for Waveform Generation

The process of calibrating a DAC for a single waveform involves finding an input sequence which produces a spectrally pure desired output waveform. This Chapter introduces an iterative technique for identifying these sequences based upon power measurements at predicted distortion frequencies. By basing the calibration on power measurements the measurement system is greatly simplified. Only noncoherent power measurements are needed to determine sequences that produce distortion free waveforms.

Section 2.1.1 outlines a procedure to minimize error noncoherently and Section 2.2 presents simulation and experimental results.

2.1 The Calibration Problem

2.1.1 Background

Given an input sequence $x(n)$, the DAC produces an output which is a combination of a signal that corresponds to the desired waveform and a signal that is error. The DAC output is given by

$$v_{DAC}(t) = x(t) + e(t) \tag{2.1}$$

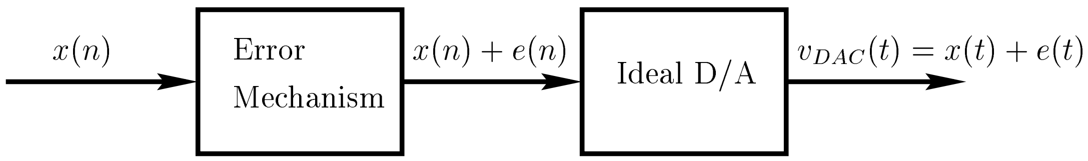

Figure 2.1: DAC model

where $x(t)$ is the ideal DAC output and $e(t)$ is an error waveform that is dependent on the input sequence. Figure 2.1 shows this DAC model. The signal $x(t)$ is assumed to be linearly related to the input sample sequence $x(n)$. The goal of DAC calibration for waveform generation is to identify a modification to the sequence which will drive $e(t)$ to zero. Let $x_m(n) = x(n) - e(n)$ denote the modified sequence, where $e(n)$ is the desired modification of the n^{th} sample.

In this section $x(n)$ (and $x(t)$) are assumed to consist of one or more narrow bandwidth components. The output $v_{DAC}(t)$ (and error sequence $e(n)$) will generally contain energy at frequencies which are not present in the input sequence due to distortion caused by the DAC. In this thesis, a noncoherent iterative technique is used to determine a sequence $e(n)$ which minimizes this distortion.

2.1.2 Determining Signal Error Noncoherently

Previous work expended much effort determining phase references between the DAC input samples and the measured samples from an ADC which is used to calibrate the DAC[1, 4, 5]. This coherent measurement system required substantial time and effort to determine the phase references. The following procedure demonstrates a method that determines the DAC error without knowledge of the timing.

The procedure is to measure the power of the DAC output at different frequencies and, based on these measurements, modify the input sequence to remove error. A laboratory setup which demonstrates the procedure is shown in Figure 2.2. The workstation/controller delivers a N_s length sequence to the pattern generator. The pattern source then cycles through the samples, repeating the sequence every $T = N_s/f_s$ seconds and the DAC translates these samples to an analog signal. This analog signal generally contains power at frequencies other than those present in $x(n)$ and the distortion power at these frequencies is then measured and

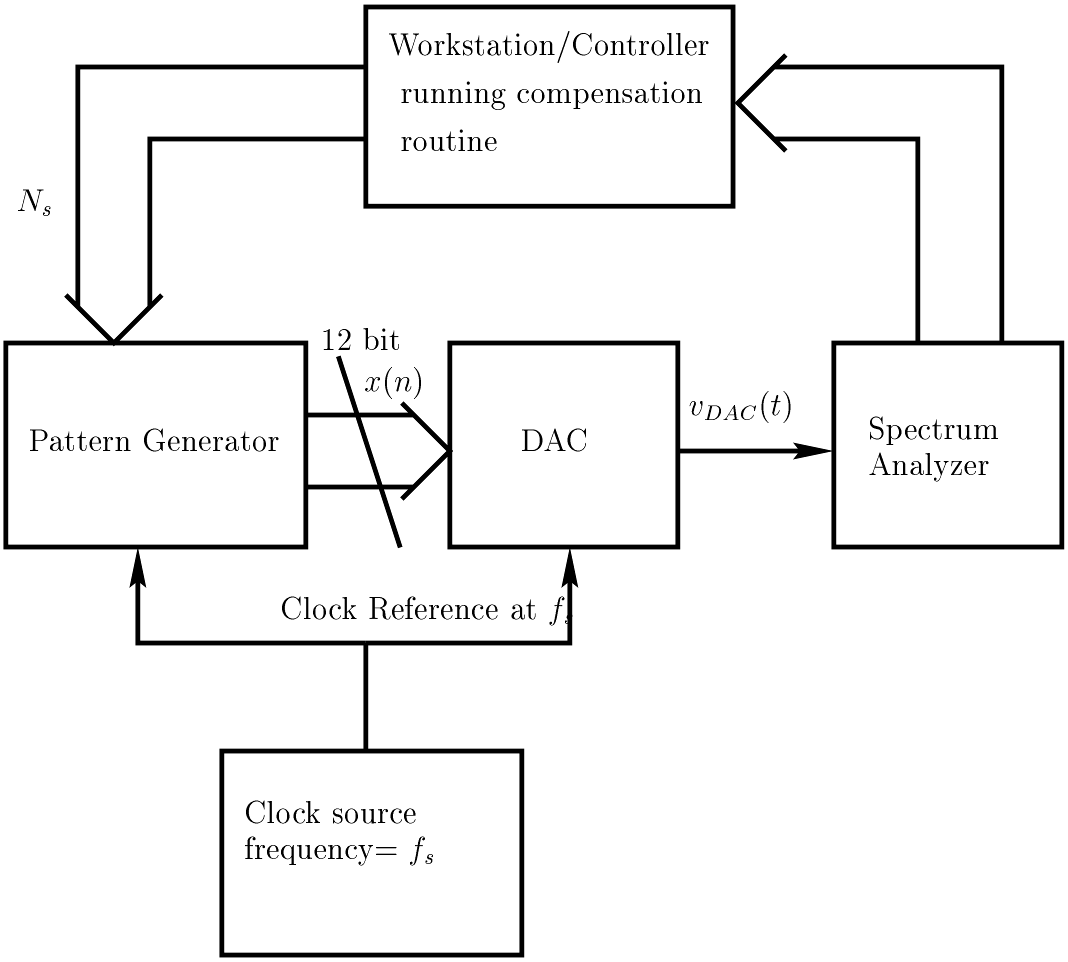

Figure 2.2: DAC setup

returned to the controller. In this thesis, a spectrum analyzer is used to perform the measurement. In practice, simpler hardware could be developed. Based on the measured values, the samples are modified and the process is repeated until the error is removed. The following analysis shows that three measurements are needed to find the desired error sequence at any given frequency. The sequence that is driving the DAC, $x(n)$, is a periodic signal since the pattern source that drives the DAC cycles through a block of data. Since $x(n)$ is periodic it has a discrete-time Fourier series(DTFS) representation

$$x(n) = \sum_{k=0}^{N_s-1} X_k e^{j2\pi kn/N_s} \tag{2.2}$$

where

$$X_k = \frac{1}{N_s} \sum_{k=0}^{N_s-1} x(n) e^{j2\pi kn/N_s}. \tag{2.3}$$

The spectrum of $x(n)$ only has N_s distinct points or *bins* for $k = 0, 1, 2, \ldots, N_s - 1$. The values of X_k represents the phase and magnitude of each spectral component. The output of an ideal DAC would contain energy only at those frequencies related to the N_s points at frequencies $f = kf_s/N_s$. To measure error, a DAC is driven with a sequence that only has energy in known bin locations. Any energy appearing in bins other than those predetermined would be considered error energy. By measuring error energy in these bins an error sequence can be determined. The error sequence also has a DTFS as in (2.2)

$$e(n) = \sum_{k=0}^{N_s-1} c_k e^{j2\pi kn/N_s}. \tag{2.4}$$

or equivalently as

$$e(n) = \sum_{k=0}^{N_s/2} a_k \cos(2\pi kn/N_s) + b_k \sin(2\pi kn/N_s), \tag{2.5}$$

where

$$|c_k|^2 = a_k^2 + b_k^2 \quad k = 0, 1, 2, \ldots, N_s - 1. \tag{2.6}$$

In order to determine the error sequence, measurements of a_k and b_k must be made. A power spectrum analyzer provides measurements of the signal power P, at the k^{th} bin. The value of P is given by $\kappa(a_k^2 + b_k^2)$ or $\kappa|c_k|^2$ where κ is a gain constant between the samples and the analog power spectrum measurement. Knowledge of a_k and b_k is desired, but not possible with one measurement. The value measured is proportional to $|c_k|^2$ and that power in the bin defines a circle on which the value of a_k and b_k must lie. The circle in Figure 2.3 is given by

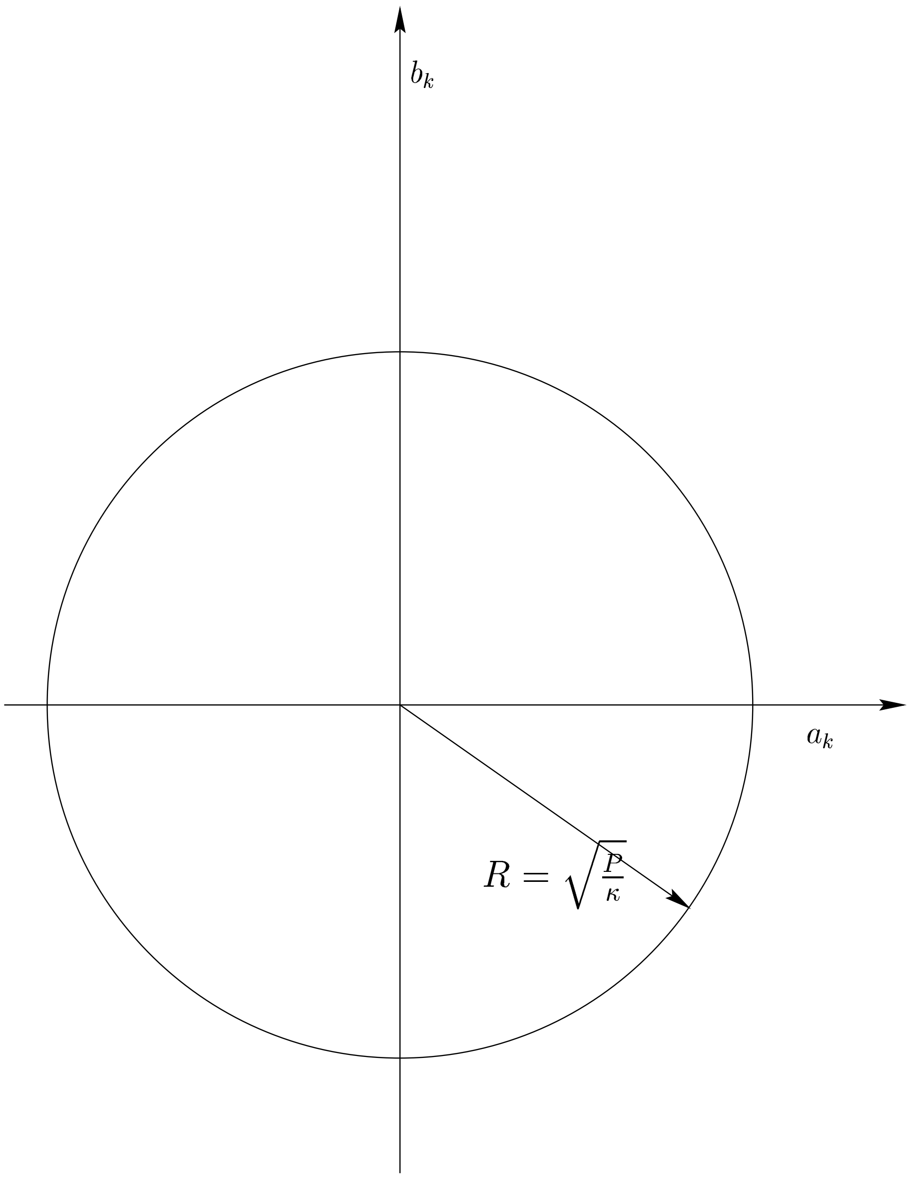

Figure 2.3: Set of possible a_k and b_k values after a single power measurement

$$R^2 = |c_k|^2 = a_k^2 + b_k^2 = \frac{P}{\kappa} \tag{2.7}$$

where R is the square root of the measured power value scaled by $\frac{1}{\sqrt{\kappa}}$. Modifying the DAC input sequence by adding a cosine with amplitude a'_k at that bin results in a change of the measured power and thus results in a new circle described by

$$R_1^2 = (a_k - a'_k)^2 + b_k^2 = \frac{P_1}{\kappa} \tag{2.8}$$

Figure 2.4 shows the addition of the second circle centered at $(a'_k, 0)$ and radius R_1. By adding this second circle, the a_k value has been identified by the intersection of the two circles since both (2.7) and (2.8) need to be satisfied and the value of b_k is narrowed to two possibilities. The exact b_k value is found by adding a sine with amplitude b'_k. This third circle has equation given by

$$R_2^2 = a_k^2 + (b_k - b'_k)^2 = \frac{P_2}{\kappa} \tag{2.9}$$

From (2.7), (2.8), and (2.9) the values of a_k and b_k can be obtained as follows:

$$a_k = \frac{R_1^2 - R^2 - a_k'^2}{-2a'_k} \tag{2.10}$$

$$b_k = \frac{R_2^2 - R^2 - b_k'^2}{-2b'_k} \tag{2.11}$$

This intersection of the three circles, at (a_k, b_k) is shown in Figure 2.5 and totally identifies the k^{th} harmonic component of the error sequence. The procedure to find error for a known waveform is as follows:

1. Drive the DAC with a signal with known amplitude to determine the scale factor κ.

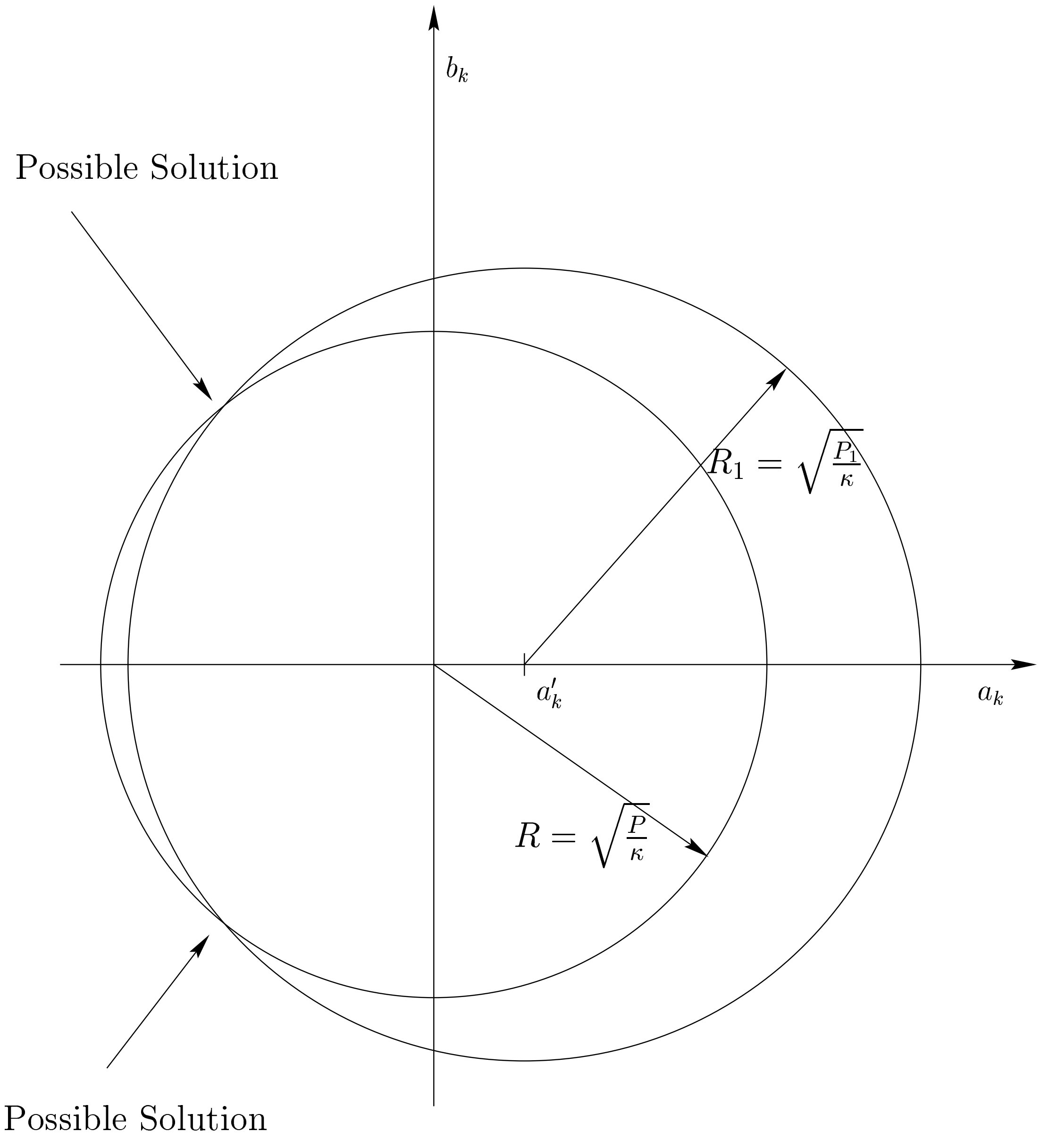

Figure 2.4: Intersection of two measures identifies a_k, and limits b_k to two values

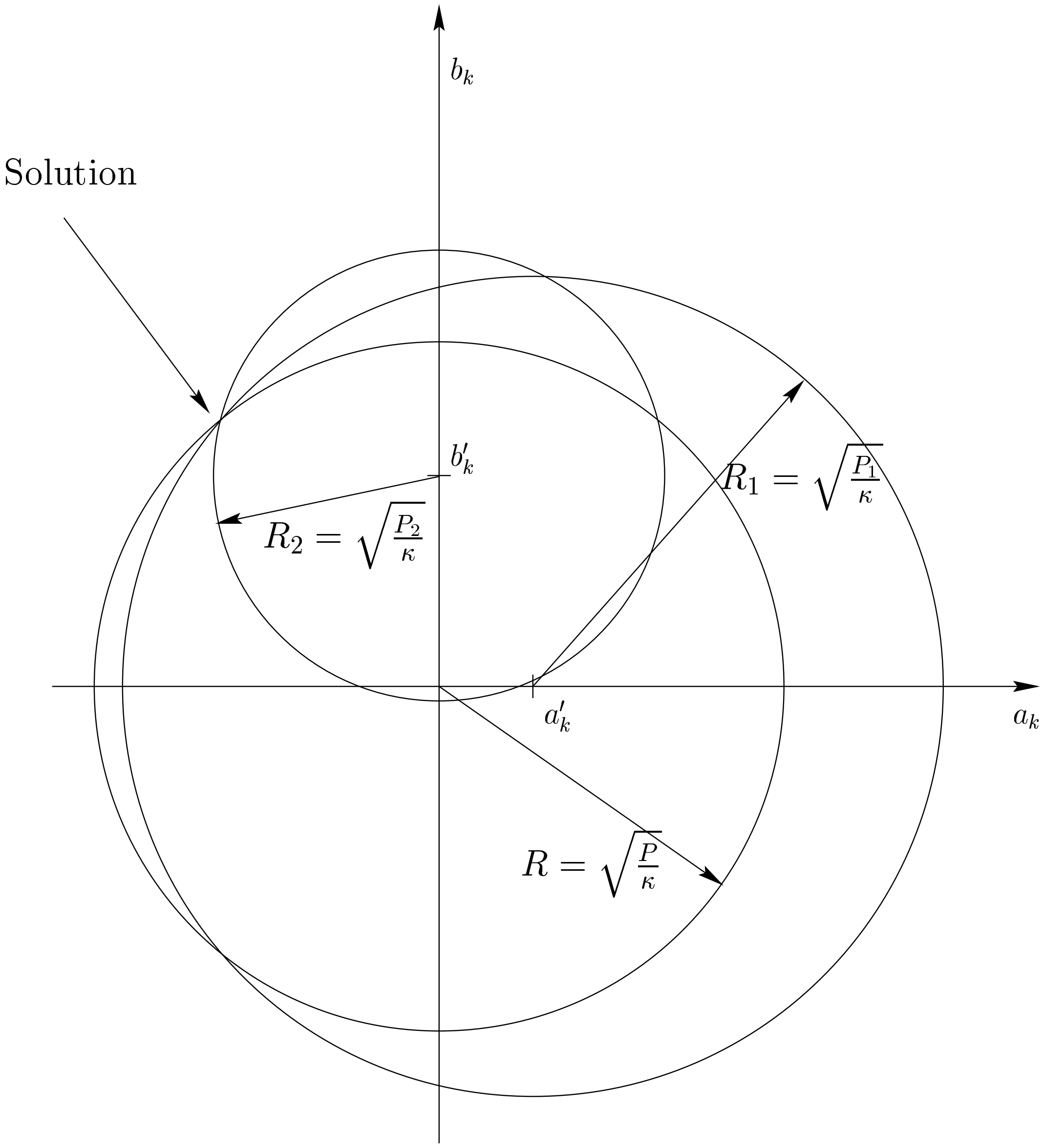

Figure 2.5: Intersection of three measures uniquely identifies a_k and b_k

2. Determine bins $\vec{b}_x = \{b_x^1\, b_x^2\, b_x^3 \ldots b_x^m\}$ and frequencies f_x on which signal energy is desired. For example, a sinewave on bin $b_x^1 = 1301$ for $N_s = 8192$ and $f_s = 102.4$ MHz corresponds to a sinewave at the output of the DAC at 16.2625 MHz.

3. Drive the DAC with a sequence which ideally produces the desired waveform.

4. Obtain power spectrum measures for $f = kf_s/N_s \quad k = 0, 1, \ldots N_s/2 - 1$.

5. Modify the original sequence by adding $\sum_{k=1}^{N_s/2-1} a'_k \cos(2\pi nk/N_s) \quad \text{for}\, k \notin \vec{b}_x$ (a_k is chosen to be 75% of $\frac{P}{\kappa}$ to guarantee an intersection).

6. Obtain power spectrum measures for first Nyquist band, $f = kf_s/N_s \quad k = 0, 1, \ldots N_s/2 - 1$.

7. Modify the original sequence by adding $\sum_{k=1}^{N_s/2-1} b'_k \sin(2\pi nk/N_s) \quad \text{for}\, k \notin \vec{b}_x$ (b_k is chosen to be 75% of $\frac{P}{\kappa}$ to guarantee an intersection).

8. Obtain power spectrum measures for $f = kf_s/N_s \quad k = 0, 1, \ldots N_s/2 - 1$.

9. Use measured values from steps 4,6, and 8 to determine estimates of a_k and b_k as in (2.10) and (2.11) and subtract from original sequence the calculated error, $\hat{e}(n) = \sum_{k=1}^{N_s/2-1} \hat{a}_k \cos(2\pi nk/N_s) + \hat{b}_k \sin(2\pi nk/N_s) \quad \text{for}\, k \notin \vec{b}_x$.

2.2 Simulated and Experimental Results

The previous section outlined a procedure to determine harmonic error in a DAC. This section will evaluate the procedure's performance on both a simulated DAC and an experimental DAC.

2.2.1 Simulation

The system involves a simulated 12-bit DAC that has a known characteristic. The DAC model consisted of a second and third order previous sample(dynamic) distortion and a second order current sample(static) distortion. The error($e(n)$) for any current sample($x(n)$) and its previous sample($x(n-1)$) is

$$e(n) = d_1x^3(n-1) + d_2x^2(n-1) + d_3x^2(n) \tag{2.12}$$

where $d_1 = 9.54 \cdot 10^{-10}$, $d_2 = 1.56 \cdot 10^{-6}$, and $d_3 = 3.91 \cdot 10^{-6}$. A two-tone signal that is useful in ADC calibration is selected as a test waveform for DAC generation. The system uses $N_s = 8192$, $f_s = 102.4$ MHz and the tones selected at bins 3903 and 3997. A full-scale signal is created and delivered to the simulated DAC producing at the output a spectrum shown in Figure 2.6. There are obvious harmonic errors being created by the DAC which the procedure should remove. Using the procedure outlined in Section 2.1.2 the signal is modified and a new sequence is delivered to the DAC that produces the output spectrum shown in Figure 2.7. This compensation has improved the spurious free dynamic range (SFDR) by approximately 25 dB. The first signal was definitely too noisy and distorted to use in ADC compensation, but the compensated signal has enough fidelity to calibrate up to a 14-bit ADC. The remaining distortion can be removed by repeating the technique starting with the modified sequence. The results of a second pass of the procedure is shown in Figure 2.8.

The new sequence produces a signal with all harmonic distortion removed, a reduction of distortion levels of over 35 dB for this simulation example.

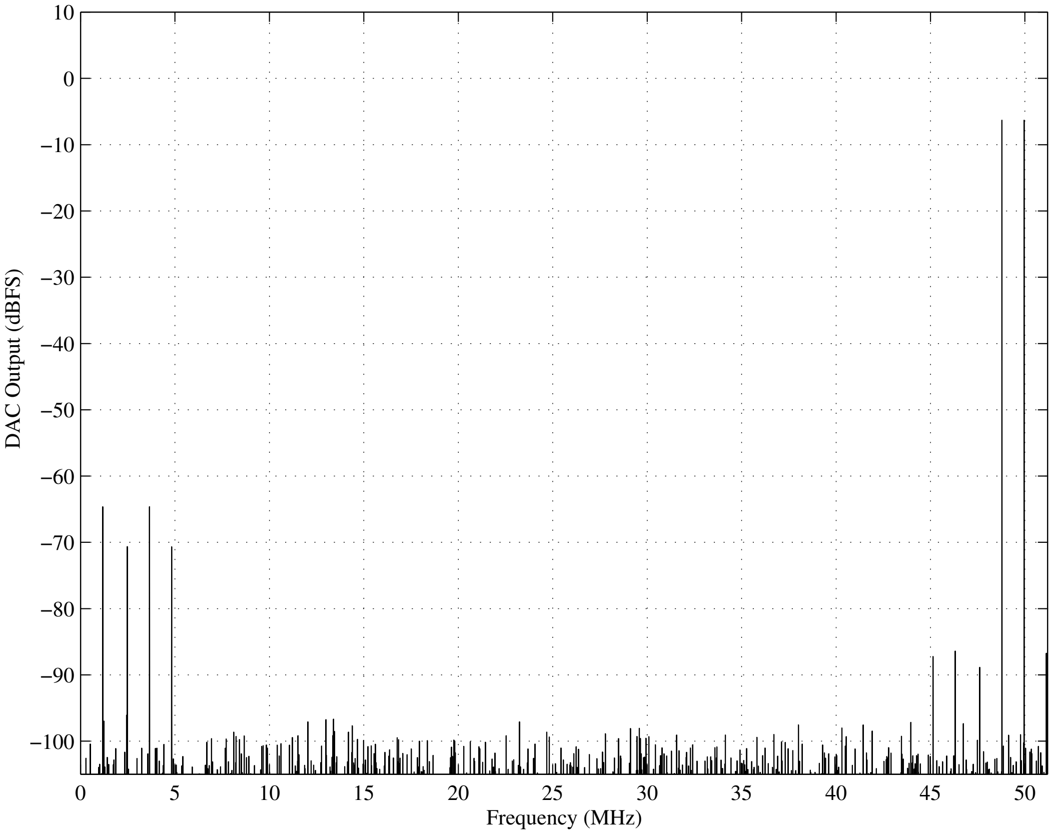

Figure 2.6: Uncompensated simulated DAC output

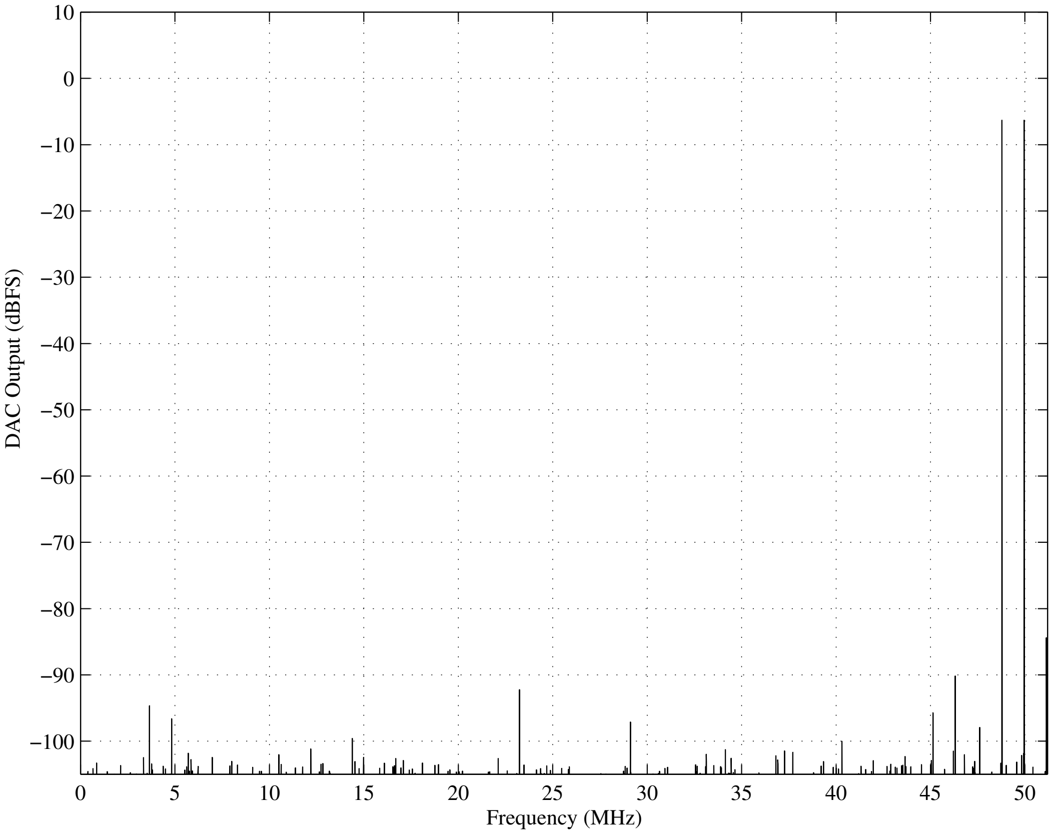

Figure 2.7: Compensated simulated DAC output, first pass

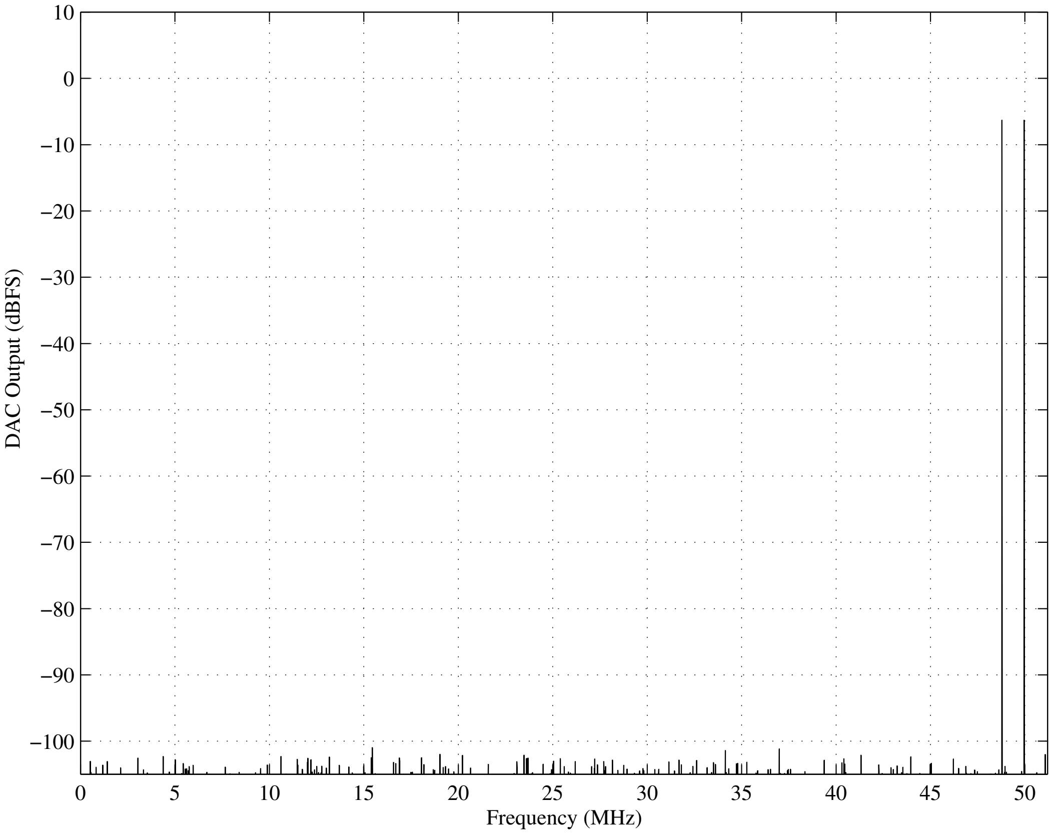

Figure 2.8: Compensated simulated DAC output, second pass

2.2.2 Experimental DAC

The procedure was tested on a Maxim MAX555 300 MSPS DAC. Figure 2.9 displays a block diagram of the experimental system. Making accurate power measurements from the spectrum analyzer requires that the analyzer be configured to provide repeatable measures. The center frequency of the analyzer is set to the desired frequency. Then the span is set to 1 kHz and the resolution bandwidth is set to 100 Hz. With this configuration a measure can be obtained reliably.

Again $N_s = 8192$, $f_s = 102.4$ MHz and a sequence with energy in bins 3903 and 3997 is used. By driving the DAC with this sequence the uncompensated spectrum shown in Figure 2.10 was obtained.

The error in the signal is significant and in its uncompensated state is unsuitable for use in ADC calibration. The procedure is applied to this sequence and the compensated result is shown in Figure 2.10. This signal has a spectrum with SFDR that is 15dB better than the uncompensated signal.

A second test using the same signal is made, however, now the output of the DAC is amplified creating additional distortion. Figure 2.11 shows the DAC output uncompensated spectrum for the amplified signal. After three iterations the harmonic and intermodulation distortion is reduced by approximately 35 dB. The new compensated output spectrum is shown in Figure 2.11.

After a single iteration, the output of the compensated DAC is not spurious free for several reasons. The first reason is that there is measurement error on the output of the DAC. A slight variance in measuring a value of power in dBm results in "leftover" error. This leftover error can be removed by applying the procedure to the new set of samples. Also changes in the sequence can yield a change in intermodulation error. These errors from changing the sequence are assumed to be negligible but, if large enough changes are made, then a change in intermodulation error can result.

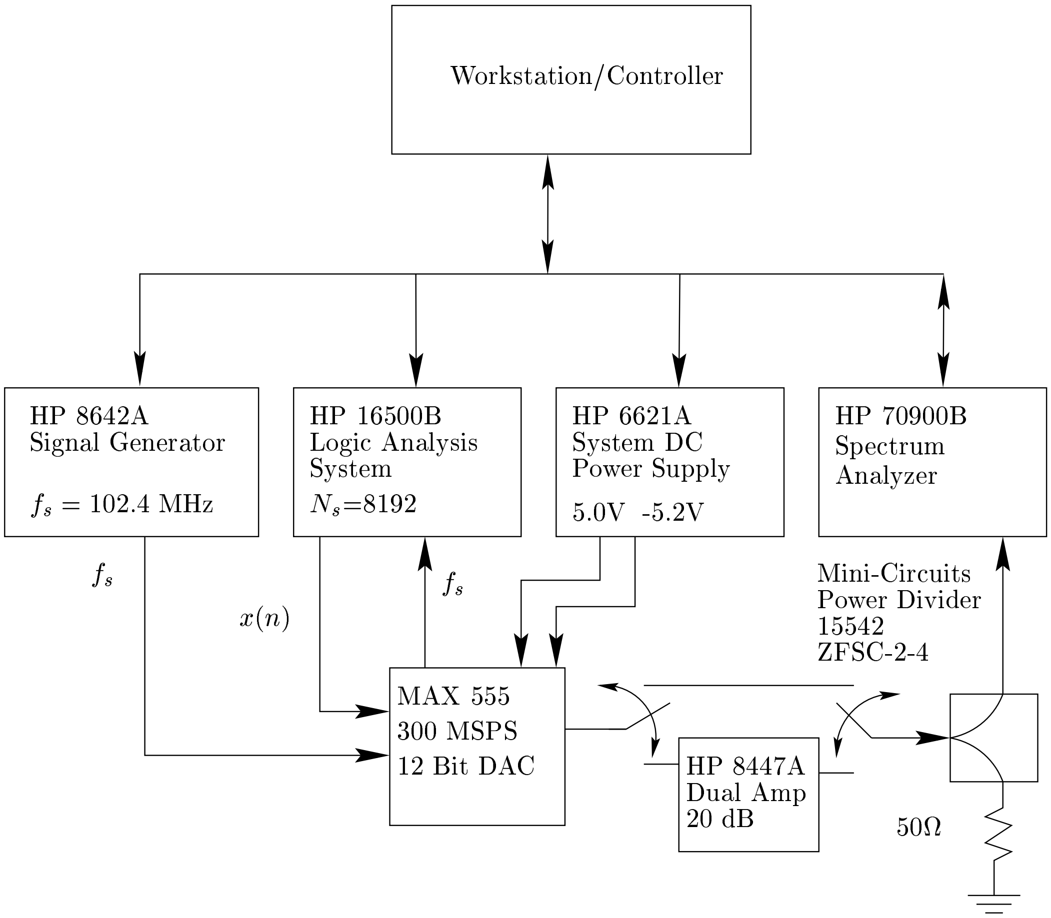

Figure 2.9: Experimental system block diagram

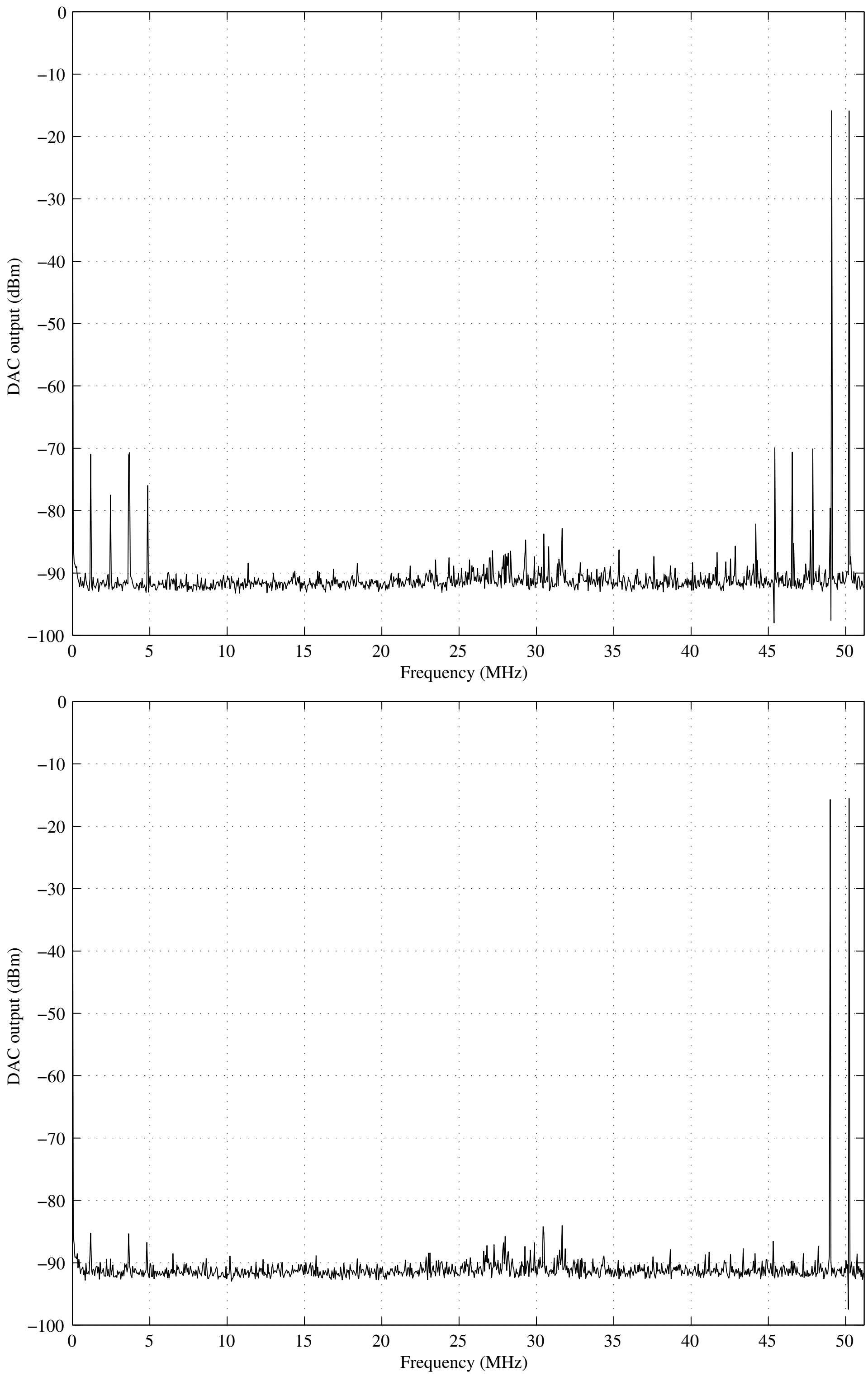

Figure 2.10: Uncompensated(top) and compensated(bottom) experimental DAC output spectrum analyzer measures

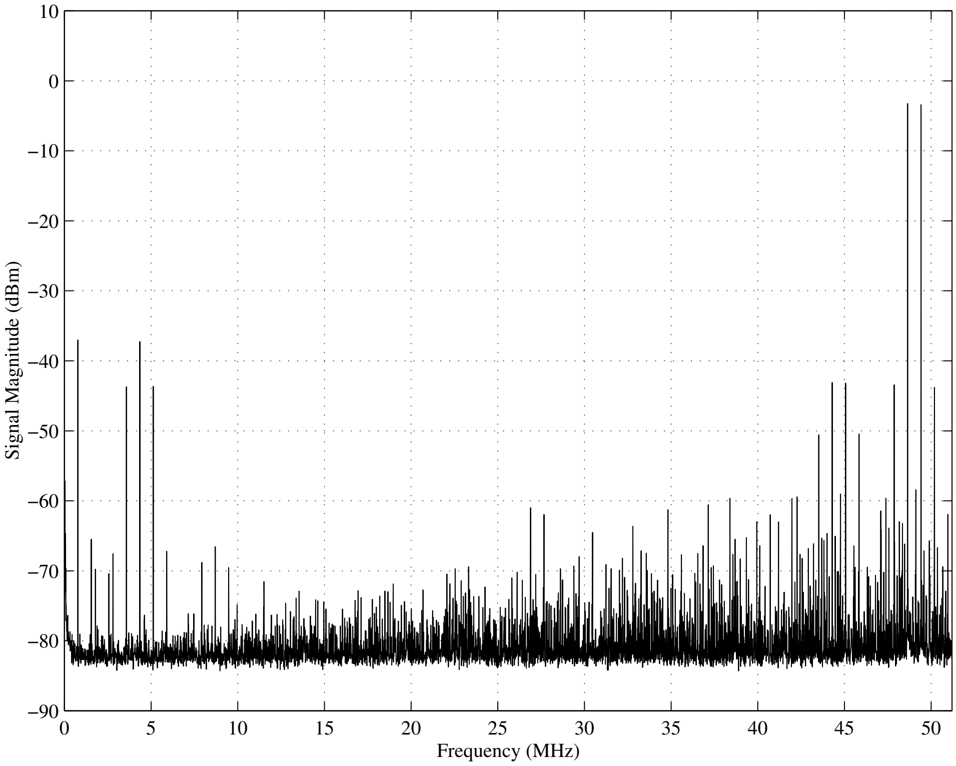

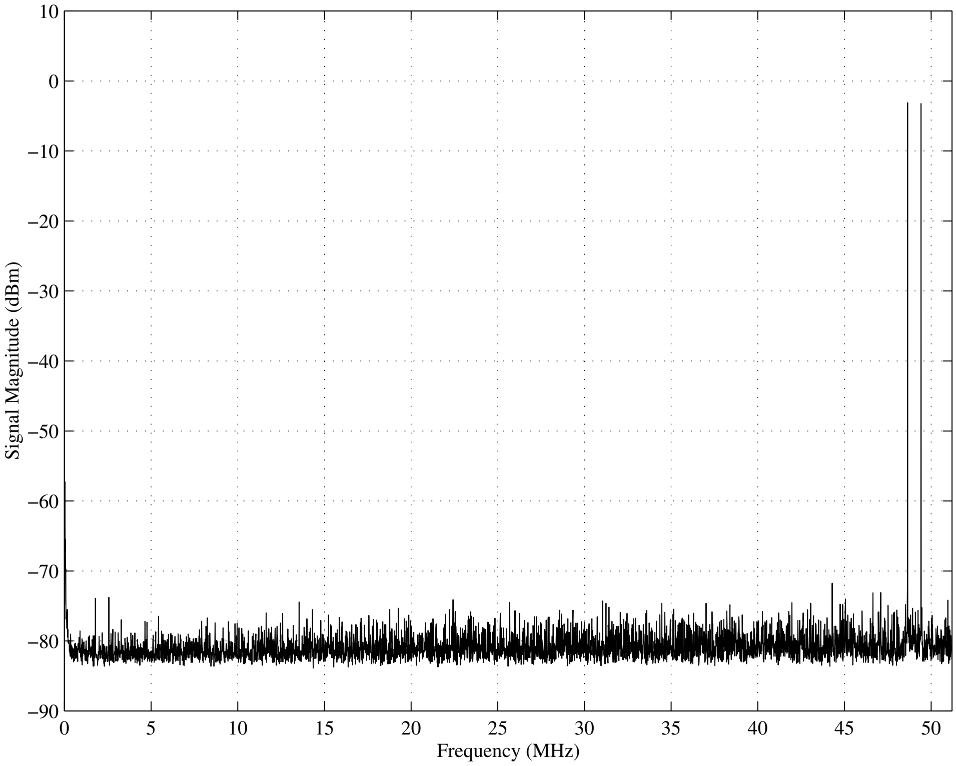

Figure 2.11: Uncompensated(top) and compensated(bottom) experimental amplified DAC output spectrum analyzer measures

CHAPTER 3

Error Generalization

Chapter 2 presented a method of determining error for a particular signal. The goal there was to remove distortion in a given waveform without concern of what caused the error. The techniques presented in Chapter 2 provide a signal that has harmonic and intermodulation distortion greatly reduced, but the technique only gives the error for an individual signal. Whether or not the knowledge of error for a particular waveform can be extended to calculate error for arbitrary waveforms, will be discussed in this chapter.

3.1 Error Models

This chapter attempts to develop a model that fits the error characteristic of the DAC, allowing error compensation for an arbitrary input signal. Previous work [1, 4, 5] has argued for using a current/previous sample model for the error in DACs and this thesis will also consider models based on current/previous sample errors. Under this model, the error for the nth sample is written as a function of the two most recent DAC input samples

$$e(n) = g\left(x(n), x(n-1)\right) \tag{3.1}$$

To determine the unknown function $g()$, a basis function representation is adopted using fixed basis functions and unknown coefficients

$$e(n) = \sum_{i=0}^{N-1} \alpha_i b_i\left(x(n), x(n-1)\right) + \epsilon. \tag{3.2}$$

The goal of DAC calibration is to solve for an appropriate set of coefficients α_i $(i = 0, 1, \ldots, N-1)$ to properly model error. In (3.2), $b_i\left(x(n), x(n-1)\right)$ denote a collection of N fixed basis functions and ϵ is the difference between the actual error sequence and the basis function expansion. For a set of N_s samples a vector representation of (3.2) may be written

$$\vec{e} = \tilde{B}\vec{\alpha} + \vec{\epsilon} \tag{3.3}$$

where $\vec{e} = \left[e(0), e(1), \ldots, e(N_s - 1)\right]^T$, $\vec{\alpha} = \left[\alpha_0, \alpha_1, \ldots, \alpha_{N-1}\right]^T$ and the (i, j) element of the matrix $\tilde{B}$ is $b_j\left(x(i), x(i-1)\right)$. The vector $\vec{\epsilon}$ denotes the modeling error.

To determine an $\vec{\alpha}$ the DAC is driven with a multi-tone calibration signal. Using the process of Chapter 2 an estimate of the harmonic components of $\vec{e}$ is obtained. With this estimate of the error $\vec{\alpha}$ can be approximated and error for other input signals can be determined using (3.2). The best set of coefficients $\vec{\alpha}$ are those that minimize the sum squared error of $\vec{\epsilon}$. With a rich enough basis set and proper coefficients, the sum squared error of $\vec{\epsilon}$ could be forced to zero. A least squares procedure is used to solve for $\vec{\alpha}$ to minimize the sum-squared error for the measurable components of $\vec{\epsilon}$. The measured error presented in Chapter 2 is not an entire representation of the error, it represents the error present at different frequencies. The measured values may be written as

$$\vec{E} = \tilde{T}\vec{e} = \tilde{T}\tilde{B}\vec{\alpha} + \tilde{T}\vec{\epsilon} \tag{3.4}$$

where $\tilde{T}$ is a linear operator given as follows

$$\tilde{T} = \begin{bmatrix} e^{0} & e^{-j2\pi(h_x^1)/N_s} & e^{-j2\pi(h_x^1)2/N_s} & \ldots & e^{-j2\pi(h_x^1)(N_s-1)/N_s} \\ e^{0} & e^{-j2\pi(h_x^2)/N_s} & e^{-j2\pi(h_x^2)2/N_s} & \ldots & e^{-j2\pi(h_x^2)(N_s-1)/N_s} \\ \vdots & \vdots & \vdots & \vdots & \vdots \\ e^{0} & e^{-j2\pi(h_x^m)/N_s} & e^{-j2\pi(h_x^m)2/N_s} & \ldots & e^{-j2\pi(h_x^m)(N_s-1)/N_s} \end{bmatrix}. \tag{3.5}$$

This does the equivalent of taking the DFT of the columns of $\tilde{B}$ and then only using the values at the m harmonic and intermodulation bin locations $\{h_x^1\, h_x^2\, h_x^3 \ldots h_x^m\}$. These distortion locations are selected to include a majority of the harmonic and intermodulation frequencies produced with a particular calibration waveform. To produce a large number of measurable distortion terms, a narrow band signal is needed as the calibration waveform. A multi-tone signal is useful to meet these requirements. The distortion terms include sum and difference of the fundamental tones. With notation

$$\tilde{T}_B = \begin{bmatrix} \mathrm{Real}\{\tilde{T}\tilde{B}\} \\ \mathrm{Imag}\{\tilde{T}\tilde{B}\} \end{bmatrix} \quad \vec{T}_e = \begin{bmatrix} \mathrm{Real}\{\tilde{T}\vec{e}\} \\ \mathrm{Imag}\{\tilde{T}\vec{e}\} \end{bmatrix} \tag{3.6}$$

a set of coefficients are found that best match the modeled harmonic error to the measured distortion. The value of $\left(\tilde{T}\vec{\epsilon}\right)^T \tilde{T}\vec{\epsilon}$ to be minimized is

$$\left(\tilde{T}\vec{\epsilon}\right)^T \tilde{T}\vec{\epsilon} = \left(\vec{T}_e - \tilde{T}_B\vec{\alpha}\right)^T \left(\vec{T}_e - \tilde{T}_B\vec{\alpha}\right) \tag{3.7}$$

$$= \vec{T}_e^T\vec{T}_e - 2\vec{T}_e^T\tilde{T}_B\vec{\alpha} + \vec{\alpha}^T\tilde{T}_B^T\tilde{T}_B\vec{\alpha}. \tag{3.8}$$

Taking the derivative with respect to $\vec{\alpha}$ and setting equal to zero gives the optimal estimate $\hat{\vec{\alpha}}$

$$\begin{aligned} \frac{d}{d\vec{\alpha}} \left(\tilde{T}\vec{\epsilon}\right)^T \tilde{T}\vec{\epsilon} &= 0 && (3.9) \\ &= 0 - 2\tilde{T}_B^T\vec{T}_e + 2\tilde{T}_B^T\tilde{T}_B\hat{\vec{\alpha}}. && (3.10) \end{aligned}$$

Solving for $\hat{\vec{\alpha}}$ yields the least-squares solution[6]

$$\hat{\vec{\alpha}} = \left(\tilde{T}_B^T\tilde{T}_B\right)^{-1} \tilde{T}_B^T\vec{T}_e. \qquad (3.11)$$

3.2 Selection of Calibration Signal

The procedure of Section 3.1 places no restrictions on the frequencies of the tones included in the calibration signal. In fact if the signal that was used to calibrate the DAC does not properly represent the range of current and previous sample inputs, then the solution will only be valid in the region of the current/previous sample space in which the calibration signal lies. To avoid a local solution and determine a global solution, a calibration signal that excites a wide range of current/previous sample combinations is desired. Previous work[1, 4, 5] determined a 6-tone waveform that would evenly cover the current/previous sample space for a 12 bit DAC. The waveform covers the current/previous sample space as shown in Figure 3.1. With this calibration waveform a solution can be obtained that will represent a large part of the error space of the DAC.

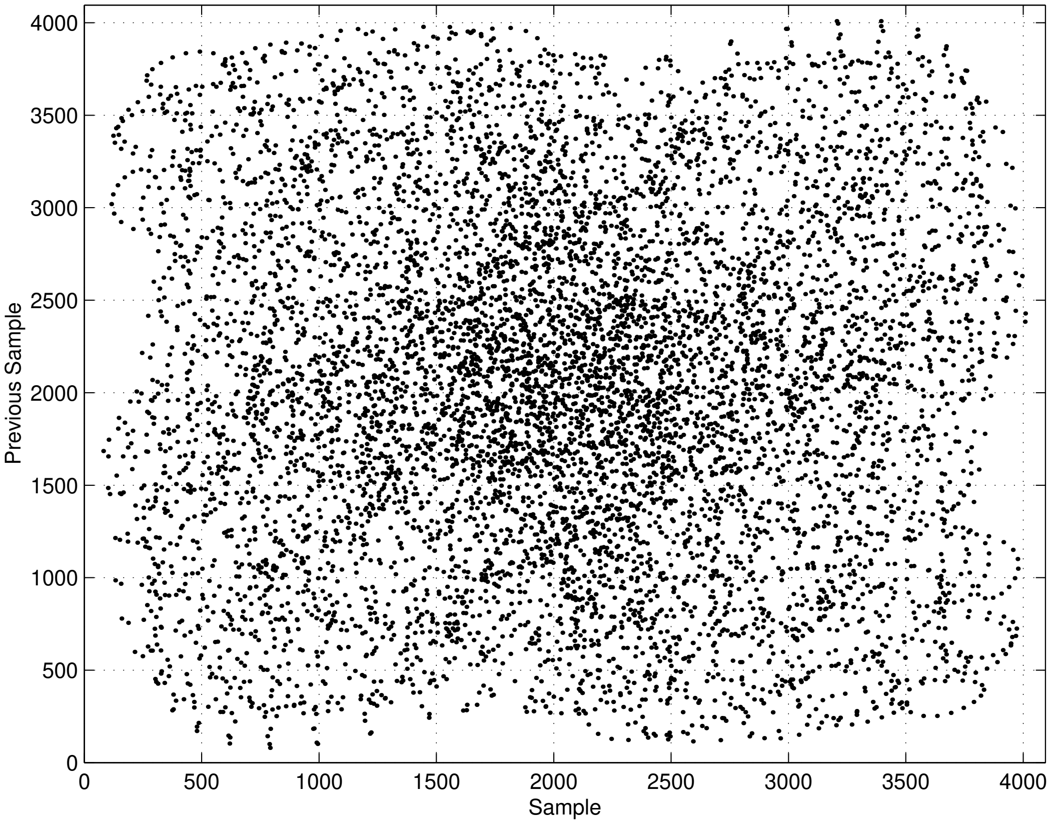

Figure 3.1: Calibration waveform for 12 bit DAC, 8192 samples

3.3 Waveform Calibration and Compensation

The procedure to determine basis coefficients is as follows:

1. Drive the DAC with a calibration waveform that covers a majority of the current/previous sample space, as shown in Figure 3.1.

2. Use the procedure outlined in Chapter 2 to obtain $\vec{e}$. The values of $\tilde{T}\vec{e}$ are then calculated by finding the DFT of $\vec{e}$ and selecting the appropriate bins $\{h_x^1\, h_x^2\, h_x^3 \ldots h_x^m\}$.

3. Evaluate basis functions at all points in the error space to obtain $\tilde{B}$. Then evaluate $\tilde{T}\tilde{B}$ by finding the DFT of each column of $\tilde{B}$ and selecting the appropriate bins $\{h_x^1\, h_x^2\, h_x^3 \ldots h_x^m\}$.

4. Separate $\tilde{T}\vec{e}$ and $\tilde{T}\tilde{B}$ into real and imaginary parts to form $\vec{T}_e$ and $\tilde{T}_B$.

5. Solve for $\hat{\vec{\alpha}} = \left(\tilde{T}_B^T \tilde{T}_B\right)^{-1} \tilde{T}_B^T \vec{T}_e$

Once the basis coefficients $\hat{\vec{\alpha}}$ are known, they can used to compensate any arbitrary DAC input sequence. The error values can be calculated from

$$\hat{e}(n) = \sum_{i=0}^{N-1} \hat{\alpha}_i b_i\left(x(n), x(n-1)\right) \tag{3.12}$$

and subtracted from the input sequence. Alternatively, the estimated error values can be stored in a lookup table by evaluating (3.12) over all possible input combinations.

3.4 Experimental Results

This section evaluates the effectiveness of the previously described calibration method. First, the algorithms are tested on a simulated DAC, then the procedure is applied to a commercially available DAC.

For the experiments, Gaussian basis functions are used. A Gaussian basis function of two variables is

$$b(x_1, x_2) = e^{-.5\left((x_1 - x_{c1})^2/\sigma_1^2 + (x_2 - x_{c2})^2/\sigma_2^2\right)}. \tag{3.13}$$

where (x_{c1}, x_{c2}) is the center and σ_1^2 and σ_2^2 are the variances for x_1 and x_2 respectively. For these experiments 49 basis functions were chosen in a 7 by 7 grid on the current/previous sample space. For a 12-bit DAC the basis function centers were chosen to be

$$\{x_{c1}, x_{c2}\} = \left\{\frac{2^{12} \cdot j}{6}, \frac{2^{12} \cdot k}{6}\right\} \qquad j, k = 0, 1, 2, 3, 4, 5, 6. \tag{3.14}$$

The variances σ_1^2 and σ_2^2 are chosen so that there is some overlap between neighboring basis functions, but not so much to make them indistinguishable. The variances were chosen to be equal ($\sigma_1^2 = \sigma_2^2 = \sigma^2$) and such that

$$\sigma = 0.1 \cdot 2^{12} \tag{3.15}$$

3.4.1 Results of Simulation

The algorithm is tested on a simulated 12-bit DAC with an error mechanism that depends on the current and previous sample. The error model of the DAC is the same as used in Chapter 2, with second and third order previous sample error and second order current sample error. The simulated DAC was driven with the six-tone calibration waveform as described by previous work[1] and the basis coefficients were determined as described in Section 3.2. To select appropriate bins $\{h_x^1\, h_x^2\, h_x^3 \ldots h_x^m\}$ the output spectrum of the DAC is examined in a large number of possible intermodulation and harmonic frequency locations. The set of bins $\{h_x^1\, h_x^2\, h_x^3 \ldots h_x^m\}$ correspond to frequencies that have error power greater than a threshold. Using $N_s = 2^{13} = 8192$ and $f_s = 102.4$ MHz, the performance of the algorithm is evaluated using three test waveforms. The first is a two equal amplitude tone signal at bin numbers 3351 and 3531 corresponding to frequencies 41.8875 MHz and 44.1375 MHz. Figure 3.2 show uncompensated and compensated spectra respectively. The uncompensated spectrum has eight measurable distortion terms. There the compensated spectrum has SFDR improved by 23 dB. The next waveform that was tested is the same two-tone signal shown in Figures 2.6 through 2.8 in Chapter 2. It is another equal amplitude two-tone signal at bins 3903 and 3997 corresponding to frequencies 48.7875 MHz and 49.9625 MHz as shown in in Figure 3.3. Again, there are a small number of measurable distortion terms in the uncompensated spectrum as shown in Figure 3.3. The improvement in SFDR using this compensation technique is comparable to the improvement obtained in Chapter 2 for the one-pass compensation, both have approximately a gain of 25 dB in SFDR. The third waveform tested was a 5-tone signal at bins 407, 3399, 3479, 3759, and 3799 corresponding to energy at frequencies 50.875, 42.4875, 43.4875 46.9875, and 47.4875 MHz. This waveform has a large number of distortion terms appearing in the uncompensated spectrum and these distortion terms were completely compensated giving a gain of 20 dB in SFDR as shown in Figure 3.4. These plots show that the algorithm is a feasible method.

3.4.2 Experimental DAC

Section 3.4.1 demonstrated that broadband DAC compensation of current/previous errors is possible from an estimated error function. This section evaluates the method on a Maxim MAX555 12-bit 300 MSPS DAC, clocked at 102.4 MHz. The experiment uses the same setup as shown in Figure 2.9. The test equipment puts a limit of using only 8192 samples. Power spectrum measurements were used to examine the output of the DAC. The same set of waveforms are used

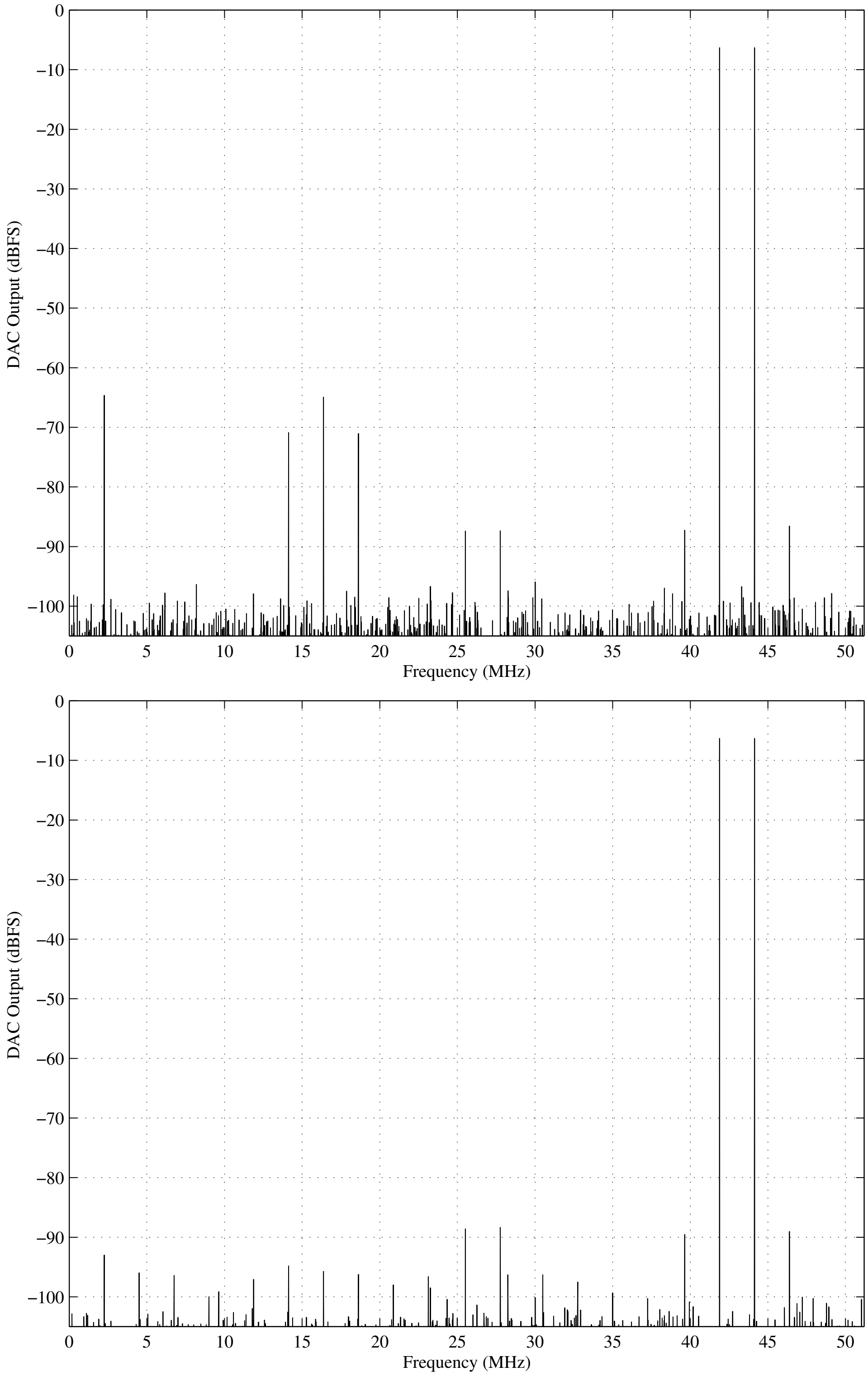

Figure 3.2: Uncompensated(top) and compensated(bottom) spectrum for a simulated DAC using a two-tone input signal with frequencies $f_1 = \frac{3351 \cdot f_s}{8192}$ MHz and $f_2 = \frac{3531 \cdot f_s}{8192}$ MHz

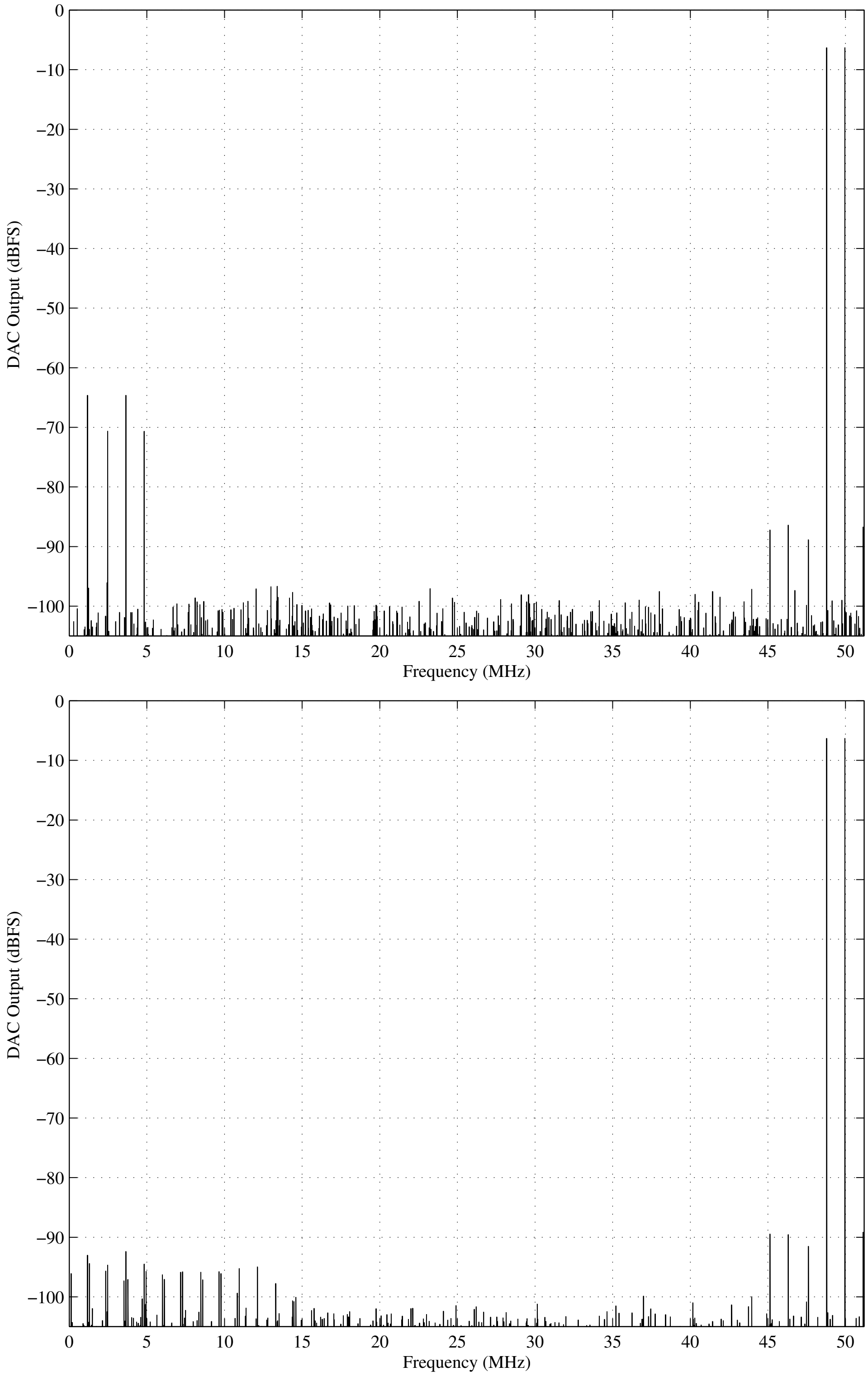

Figure 3.3: Uncompensated(top) and compensated(bottom) spectrum for a simulated DAC using a two-tone input signal with frequencies $f_1 = \frac{3903 \cdot f_s}{8192}$ MHz and $f_2 = \frac{3799 \cdot f_s}{8192}$ MHz

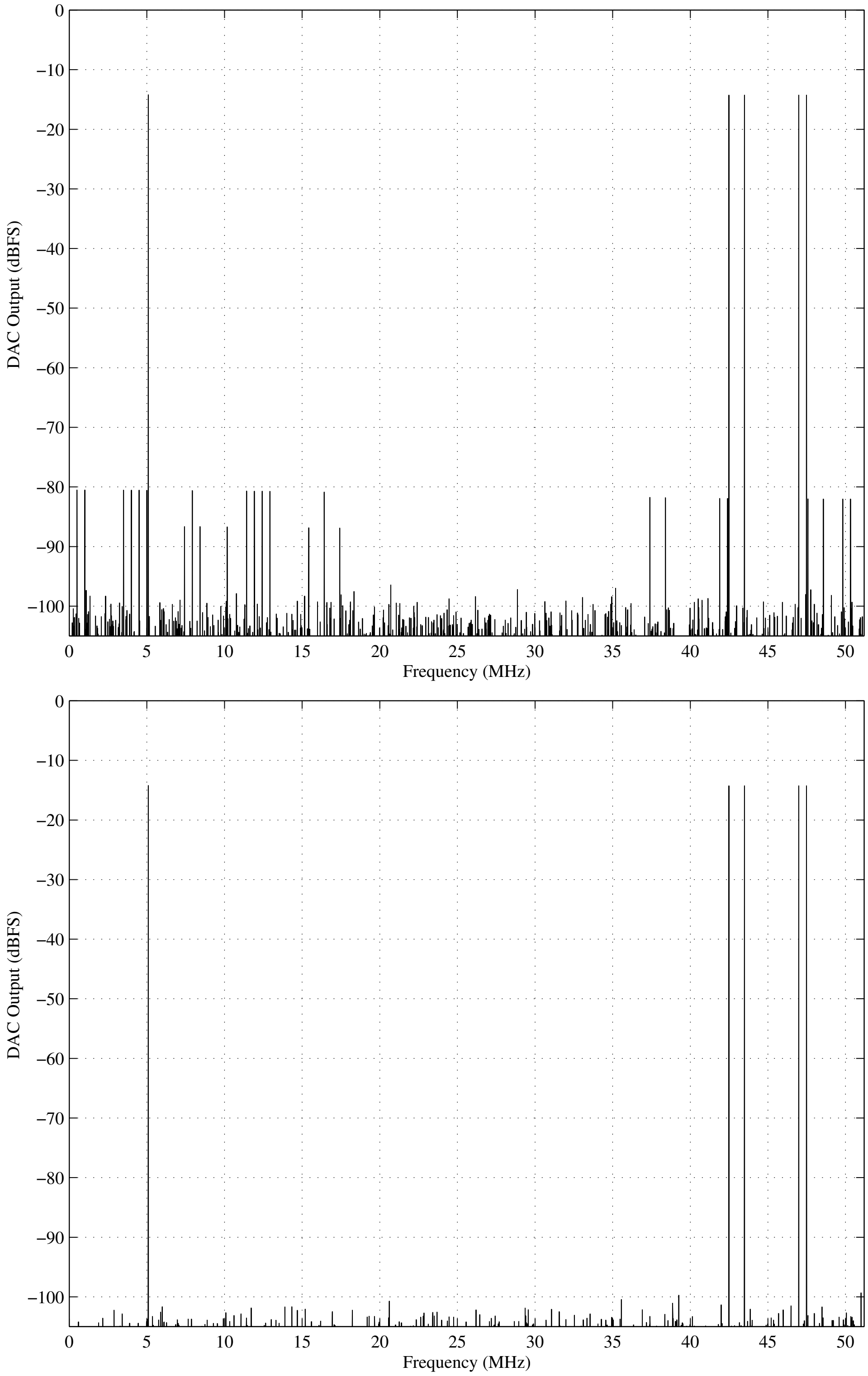

Figure 3.4: Uncompensated(top) and compensated(bottom) spectrum for a simulated DAC using a five-tone input signal with frequencies $f_1 = \frac{407 \cdot f_s}{8192}$ MHz and $f_2 = \frac{3399 \cdot f_s}{8192}$ MHz $f_3 = \frac{3479 \cdot f_s}{8192}$ MHz $f_4 = \frac{3759 \cdot f_s}{8192}$ MHz $f_5 = \frac{3799 \cdot f_s}{8192}$ MHz

as in the simulation. Figures 3.5 through 3.7 show the measured uncompensated and compensated spectra of three waveforms respectively. It is clear that the compensation did not perform as predicted by simulation. In fact, the compensation failed to improve the SFDR in all three cases, only minor improvements in smaller harmonic components was achieved. The compensation routine also failed to compensate the calibration waveform. Insight into these failures will be explored in Chapter 4.

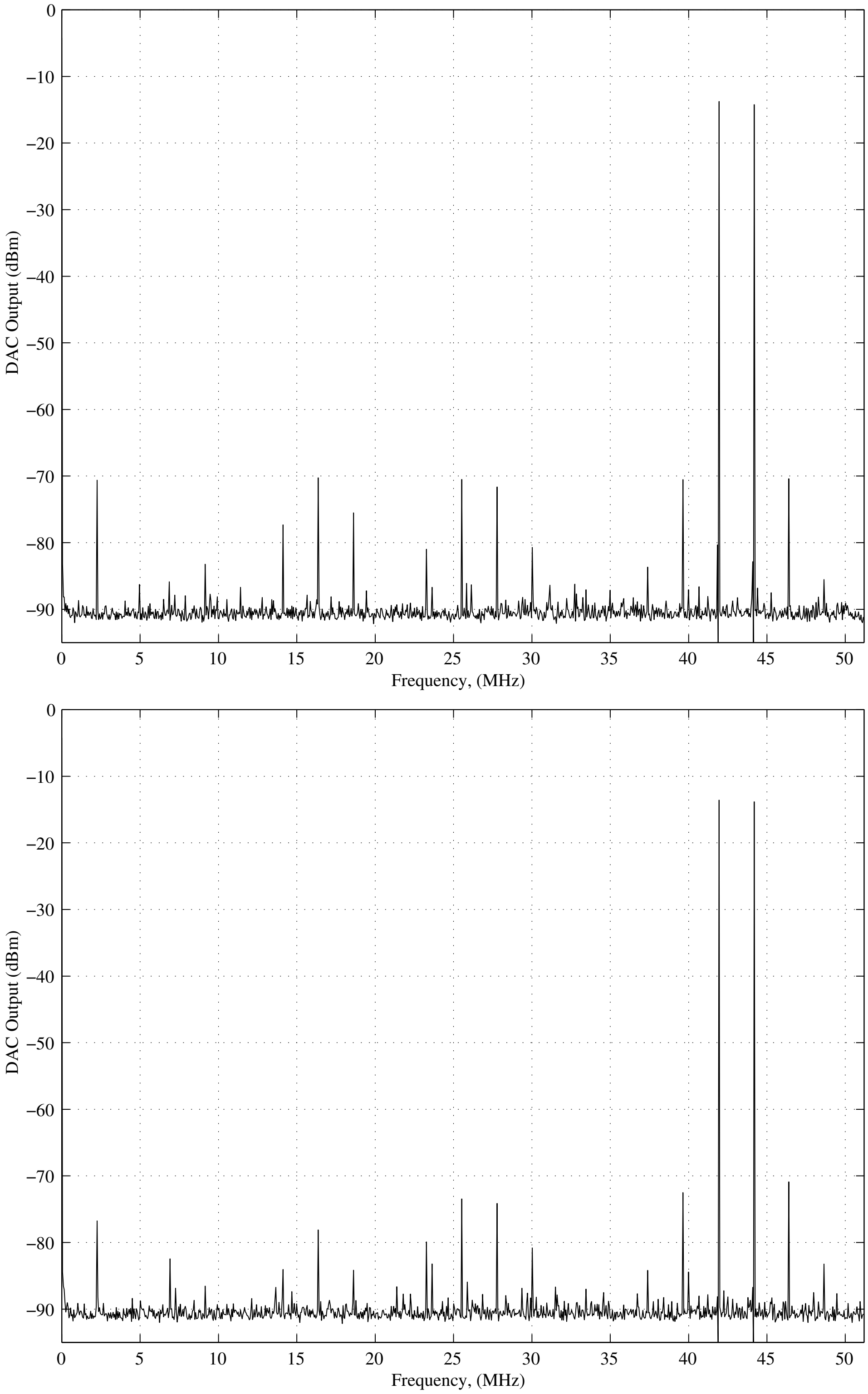

Figure 3.5: Uncompensated(top) and compensated(bottom) spectrum for an experimental DAC using a two-tone input signal with frequencies $f_1 = \frac{3351 \cdot f_s}{8192}$ MHz and $f_2 = \frac{3531 \cdot f_s}{8192}$ MHz

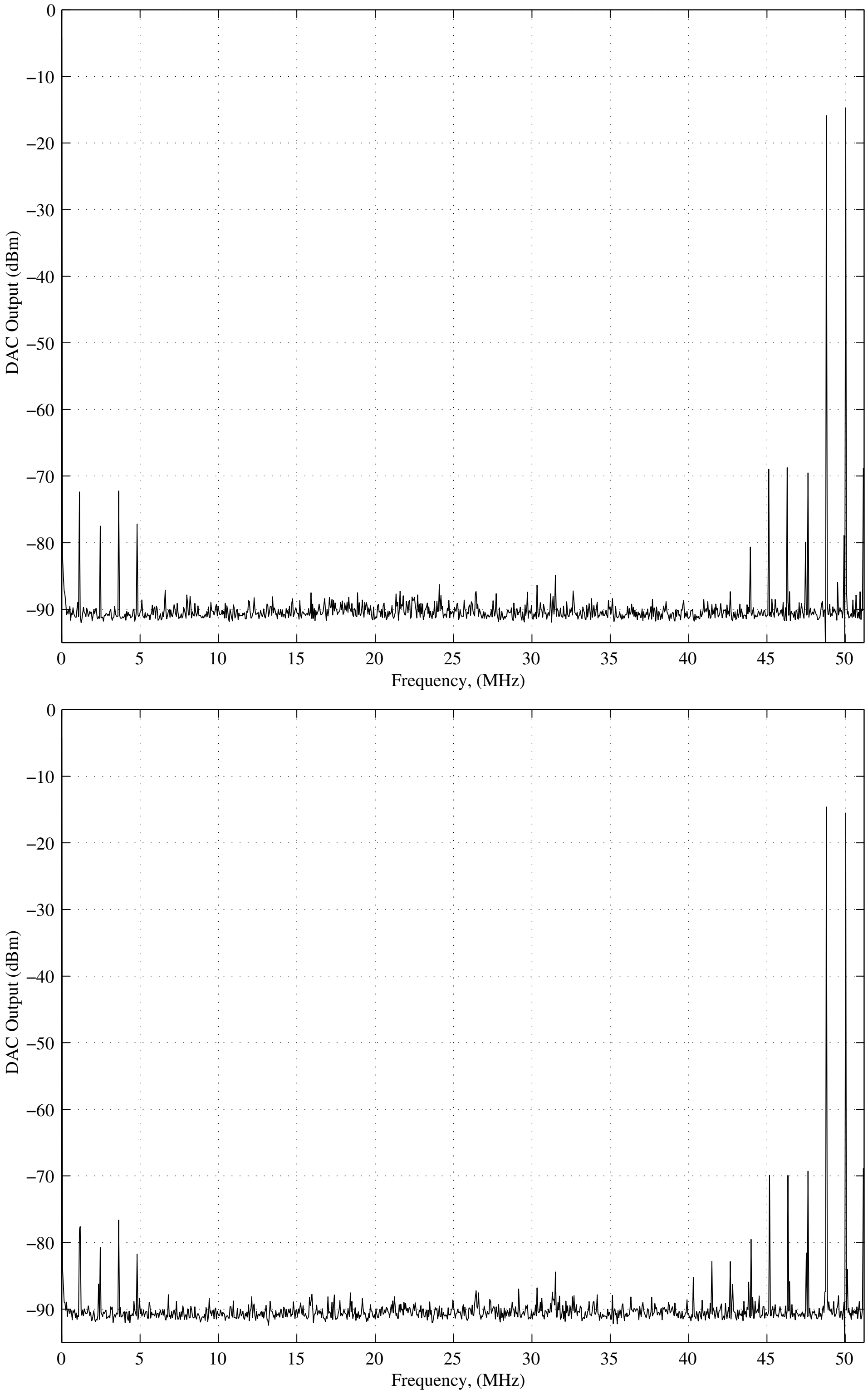

Figure 3.6: Uncompensated(top) and compensated(bottom) spectrum for an experimental DAC using a two-tone input signal with frequencies $f_1 = \frac{3903 \cdot f_s}{8192}$ MHz and $f_2 = \frac{3799 \cdot f_s}{8192}$ MHz

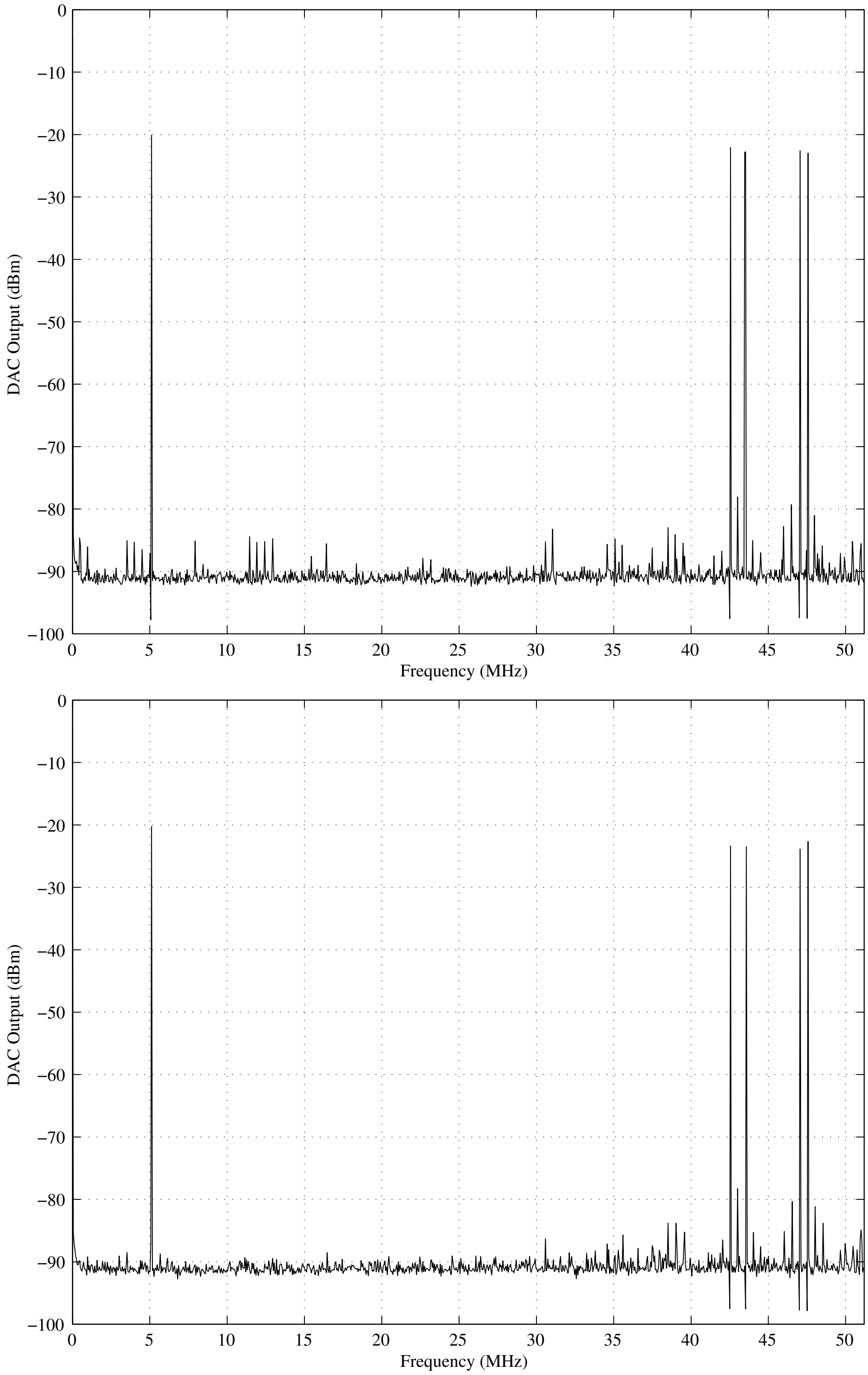

Figure 3.7: Uncompensated(top) and compensated(bottom) spectrum for an experimental DAC using a five-tone input signal with frequencies $f_1 = \frac{407 \cdot f_s}{8192}$ MHz and $f_2 = \frac{3399 \cdot f_s}{8192}$ MHz $f_3 = \frac{3479 \cdot f_s}{8192}$ MHz $f_4 = \frac{3759 \cdot f_s}{8192}$ MHz $f_5 = \frac{3799 \cdot f_s}{8192}$ MHz

CHAPTER 4

Discussion of Results

Chapter 3 presented a DAC compensation technique which performed well in simulation, but poorly for the experimental DAC. This chapter examines possible causes of failure.

4.1 Failure of Excitation

One possible cause of the experimental DAC failure could be a failure to excite the error mechanisms enough to be measured. A six tone signal has many possible intermodulation terms and the error power is spread among them. Some of that error may not be measured correctly or at all if the error at a particular frequency is below the noise floor. In simulation, many error terms appear above the noise floor and the compensation algorithm includes them in the solution. The solution is valid when the measured distortion accurately represents the error characteristic of the device. It is not possible to lower the noise floor on the experimental DAC to measure smaller error terms. Therefore another calibration waveform must be used to provide measurable error terms. Any signal that is to be used in calibration must cover the current/previous sample space and usually this requires a multi-tone signal. Any single multi-tone signal that adequately covers this space will likely present a similar problem as the previously used 6-tone signal. By using a set of three two-tone signals the current/previous sample space is adequately covered. These two-tone signals will have many fewer but stronger intermodulation terms in which to spread the error power thereby providing measurable error terms. Figure 4.1 shows how the three two-tone signals cover the current/previous sample space.

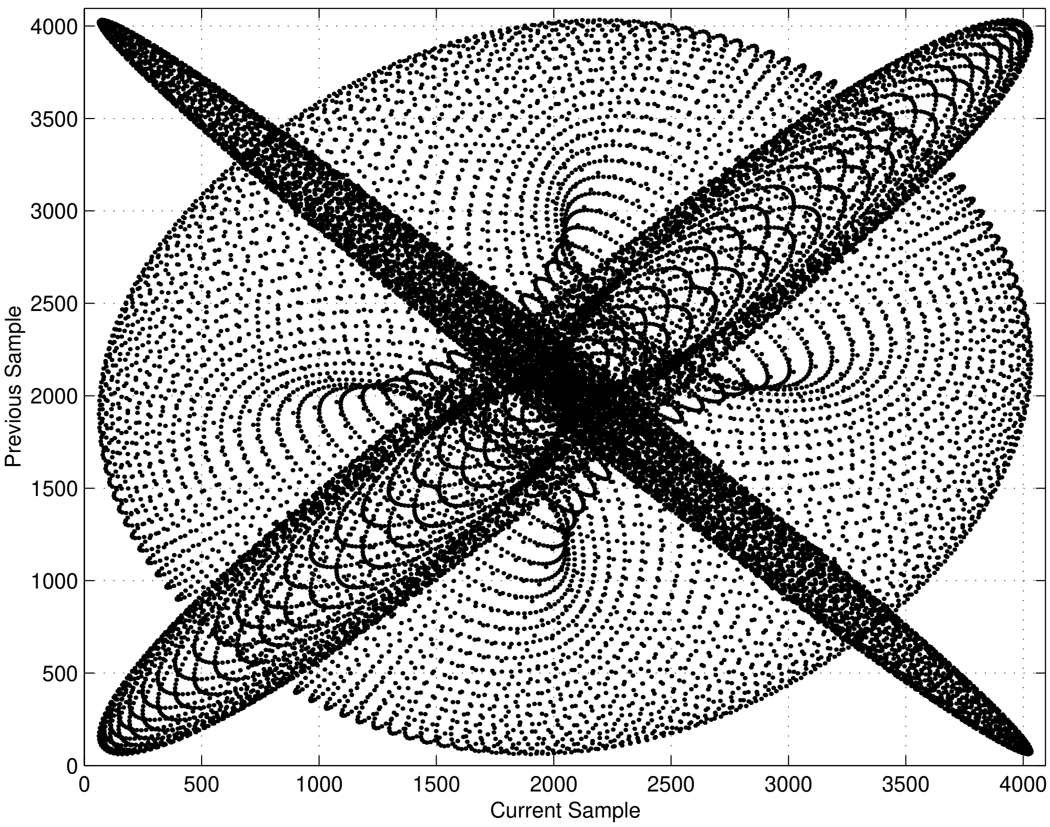

Figure 4.1: Coverage of the current/previous sample space using a set of three two-tone signals

The calibration process when using the three two-tone signals has two small changes. When solving for the basis coefficients $\vec{\alpha}$, the information from all the three signals must be included. Chapter 3 showed

$$\hat{\vec{\alpha}} = \left(\tilde{T}_B^T \tilde{T}_B\right)^{-1} \tilde{T}_B^T \vec{T}_e \tag{4.1}$$

The only changes are in $\tilde{T}_B$ and $\vec{T}_e$. For each waveform they are calculated and then combined as follows

$$\tilde{T}_B = \begin{bmatrix} \tilde{T}_{B1} \\ \tilde{T}_{B2} \\ \tilde{T}_{B3} \end{bmatrix} \quad \tilde{T}_e = \begin{bmatrix} \tilde{T}_{e1} \\ \tilde{T}_{e2} \\ \tilde{T}_{e3} \end{bmatrix} \tag{4.2}$$

With these modifications, the compensation algorithm is again tested in simulation. For calibration of the simulated DAC, three two-tone signals located on bins 1351 and 2531, 3903 and 3997, 101 and 577 are used(for $N_s = 8192$). The calibration is evaluated by using the estimated $\vec{\alpha}$ to compensate three different signals, a two-tone, a five-tone and a three-tone signal. Figures 4.2 through 4.4 show simulated uncompensated and compensated spectra. The compensation routine reduces the harmonic distortion by 20, 10 and 15 dB respectively. The remaining distortion is a result of the test signal not lying inside the calibration space. The calibration waveforms do not completely cover the current/previous sample space and thereby cannot correctly model the distortion in some areas of the space. This inaccuracy is a not a major concern as there is still a great reduction in spurious tones.

This simulation demonstrates that it is feasible to use several two-tone signals to calibrate the DAC and therefore the technique is now applied to the experimental DAC. The experimental DAC is calibrated and tested using the same waveforms as in simulation. Figures 4.5 through 4.7 show results for two-tone cal-

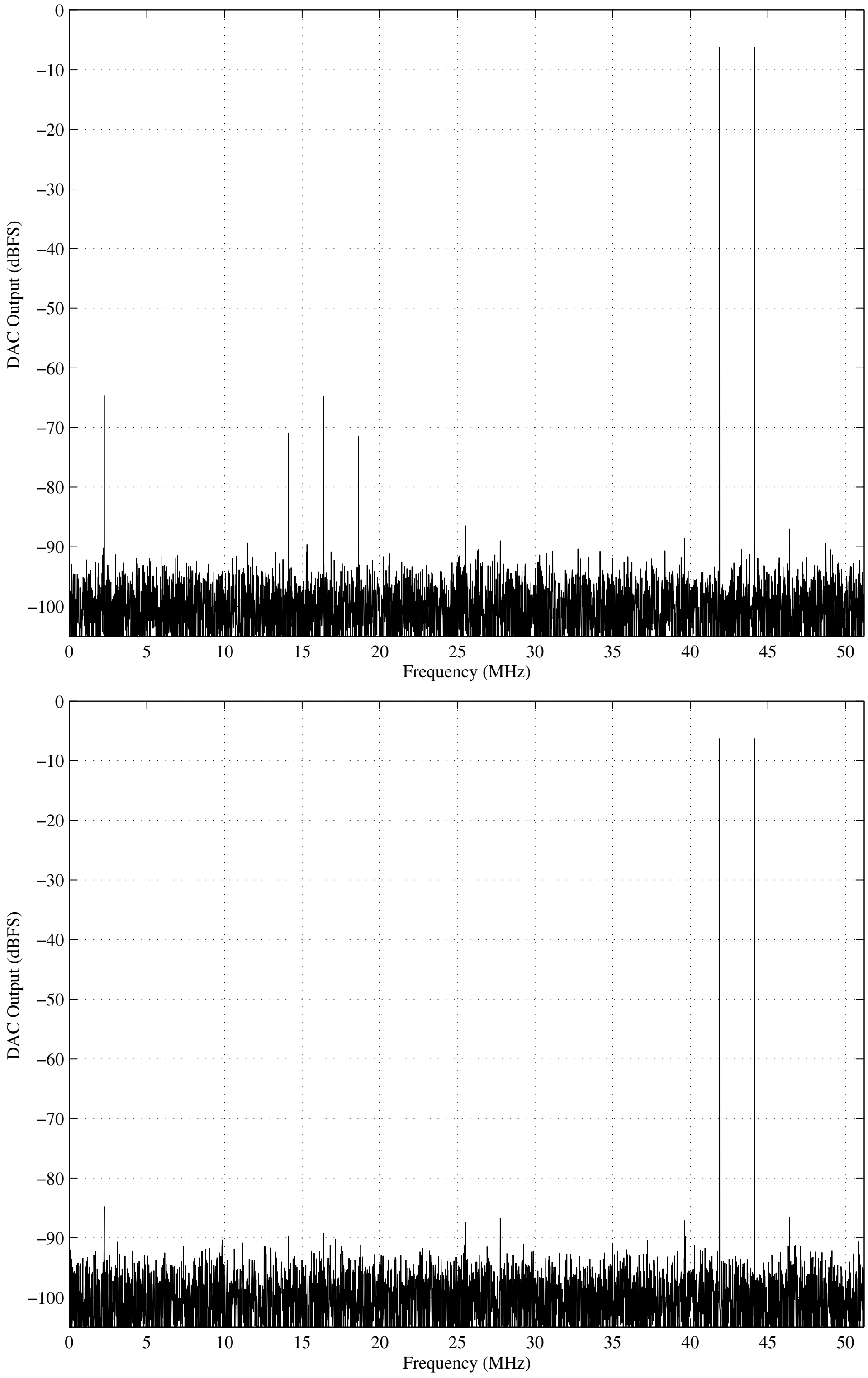

Figure 4.2: Uncompensated(top) and compensated(bottom) simulated spectrum using three two-tone calibration, two-tone test signal at frequencies $f_1 = \frac{3351 \cdot f_s}{8192}$ and $f_2 = \frac{3531 \cdot f_s}{8192}$

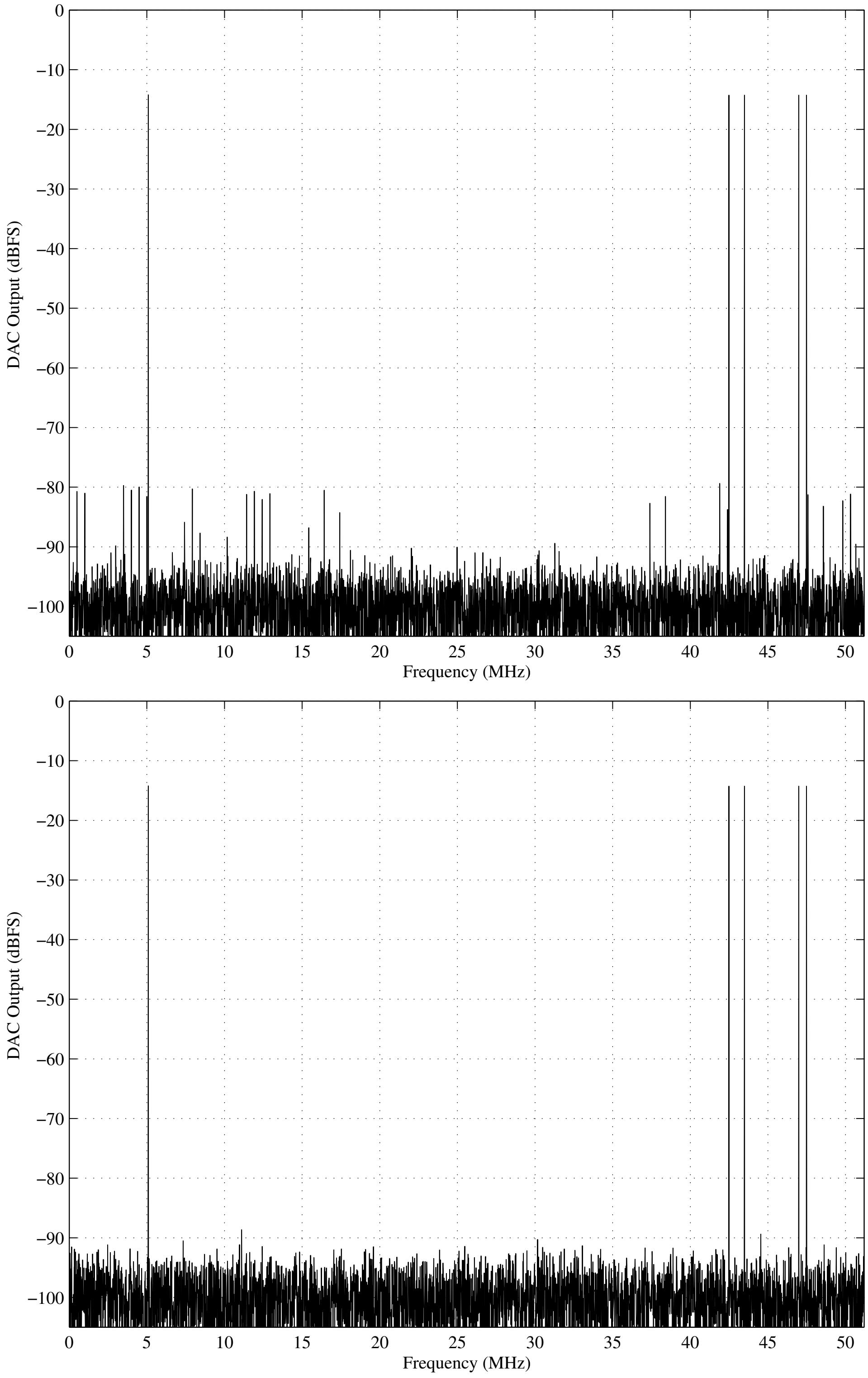

Figure 4.3: Uncompensated(top) and compensated(bottom) simulated spectrum using three two-tone calibration, five-tone test signal at frequencies $f_1 = \frac{407 \cdot f_s}{8192}$, $f_2 = \frac{3399 \cdot f_s}{8192}$, $f_3 = \frac{3479 \cdot f_s}{8192}$, $f_4 = \frac{3759 \cdot f_s}{8192}$, and $f_5 = \frac{3799 \cdot f_s}{8192}$

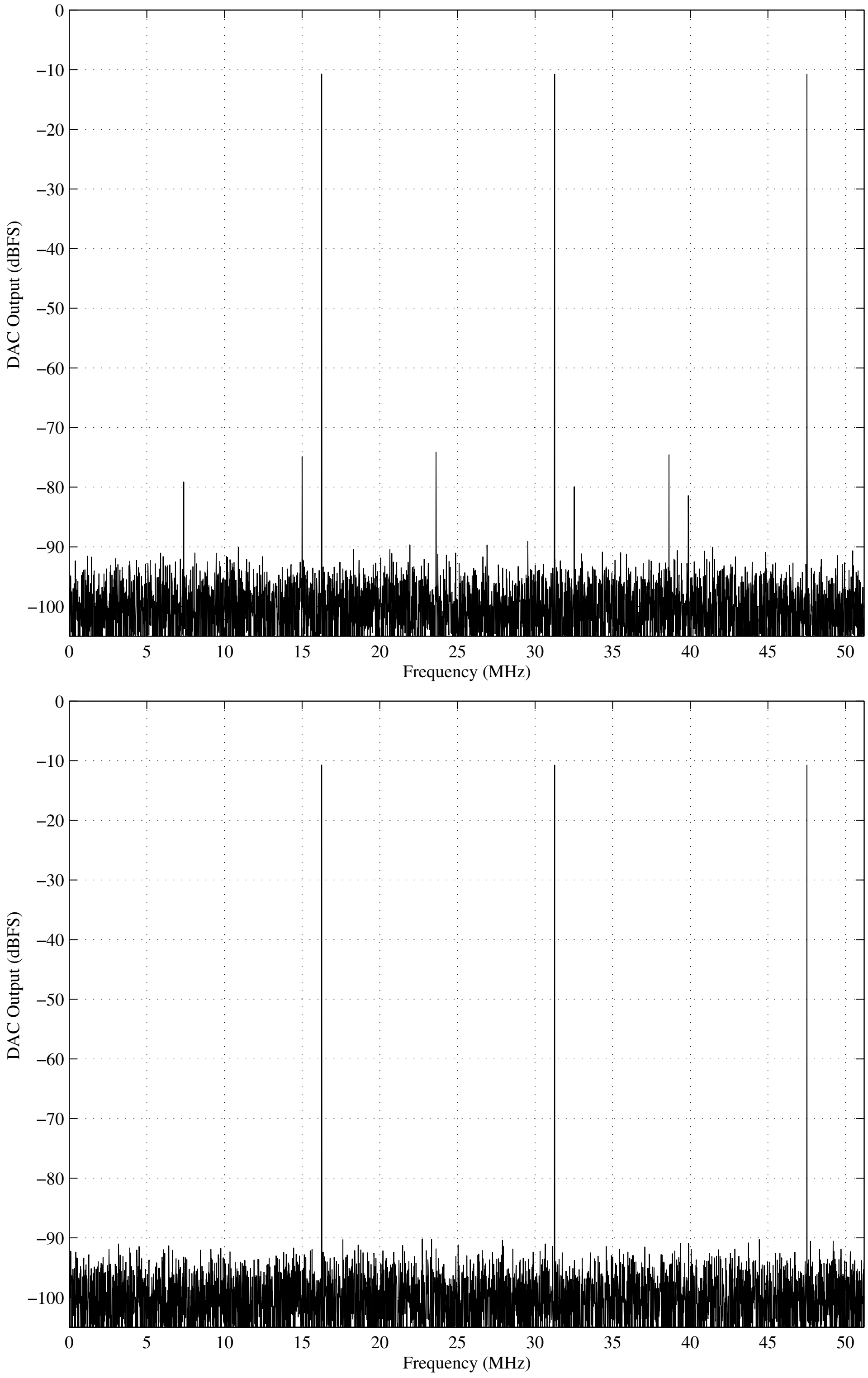

Figure 4.4: Uncompensated(top) and compensated(bottom) simulated spectrum using three two-tone calibration, three-tone test signal at frequencies $f_1 = \frac{1301 \cdot f_s}{8192}$, $f_2 = \frac{2501 \cdot f_s}{8192}$, and $f_3 = \frac{3801 \cdot f_s}{8192}$

ibration. From these figures it is obvious that the compensation was unsuccessful, and since there is measurable error in the calibration with these waveforms, it stands to reason that there is another cause of failure.

4.2 Error in Modeling

Section 4.1 demonstrated that failure to excite the error mechanism was not the cause of failure. Another possible cause for failure is a mistake in modeling. Previous work[1, 4, 5] argued that the error in a DAC was a function of the current and the previous sample, therefore the basis functions were selected as functions of the current and previous sample. If the error in the DAC is a function of something else, then the calibration would not correctly model the error and compensation would be impossible using this model.

One error mechanism that has been thought to be a function of the current and previous sample is slew-limiting. Slew-limiting is simply the DAC's inability to instantaneously change state. There is a finite rate at which the DAC output can change. In simulation the DAC error is made to be a function of the current and previous sample to test the algorithms, but this section looks at a simulation which models the analog output of the DAC with slew limit effect. To model this effect the DAC output samples are oversampled by a factor of 128. This simply means inserting 127 points between each DAC output sample. This creates an approximation to an "analog" waveform that has many more points than the original but carries the same information. Figure 4.8 shows a zoomed section of an oversampled waveform. The waveform has been slew-limited, and its effect is to create the samples between desired current and previous output values. The slew-limiting mechanism causes the output of the simulated DAC to not jump from the previous sample to the current sample. Instead, the DAC output ramps up to the current sample at a constant slope. The simulated DAC model slew-limit

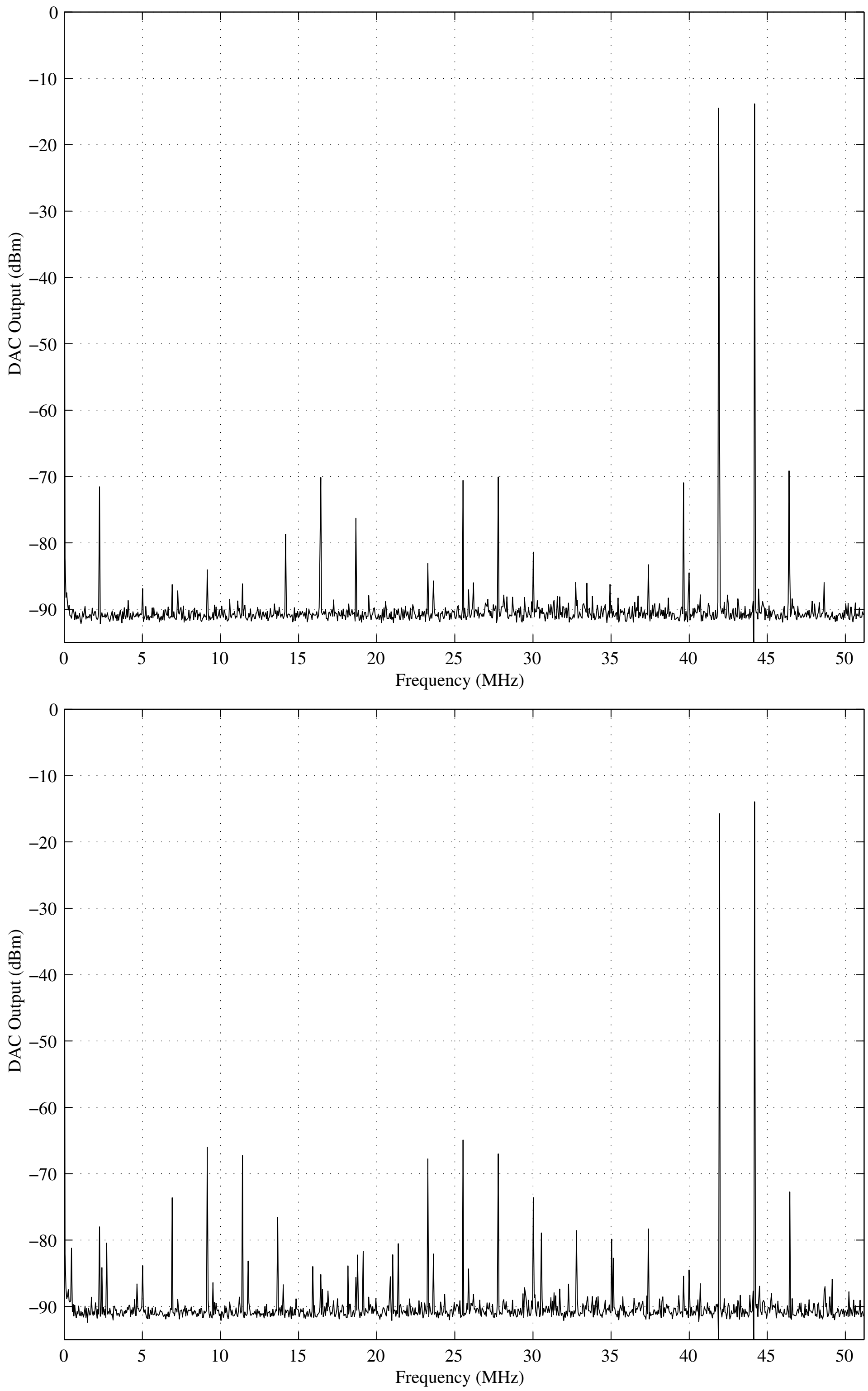

Figure 4.5: Uncompensated(top) and compensated(bottom) spectrum using three two-tone calibration, two-tone test signal at frequencies $f_1 = \frac{3351 \cdot f_s}{8192}$ and $f_2 = \frac{3531 \cdot f_s}{8192}$

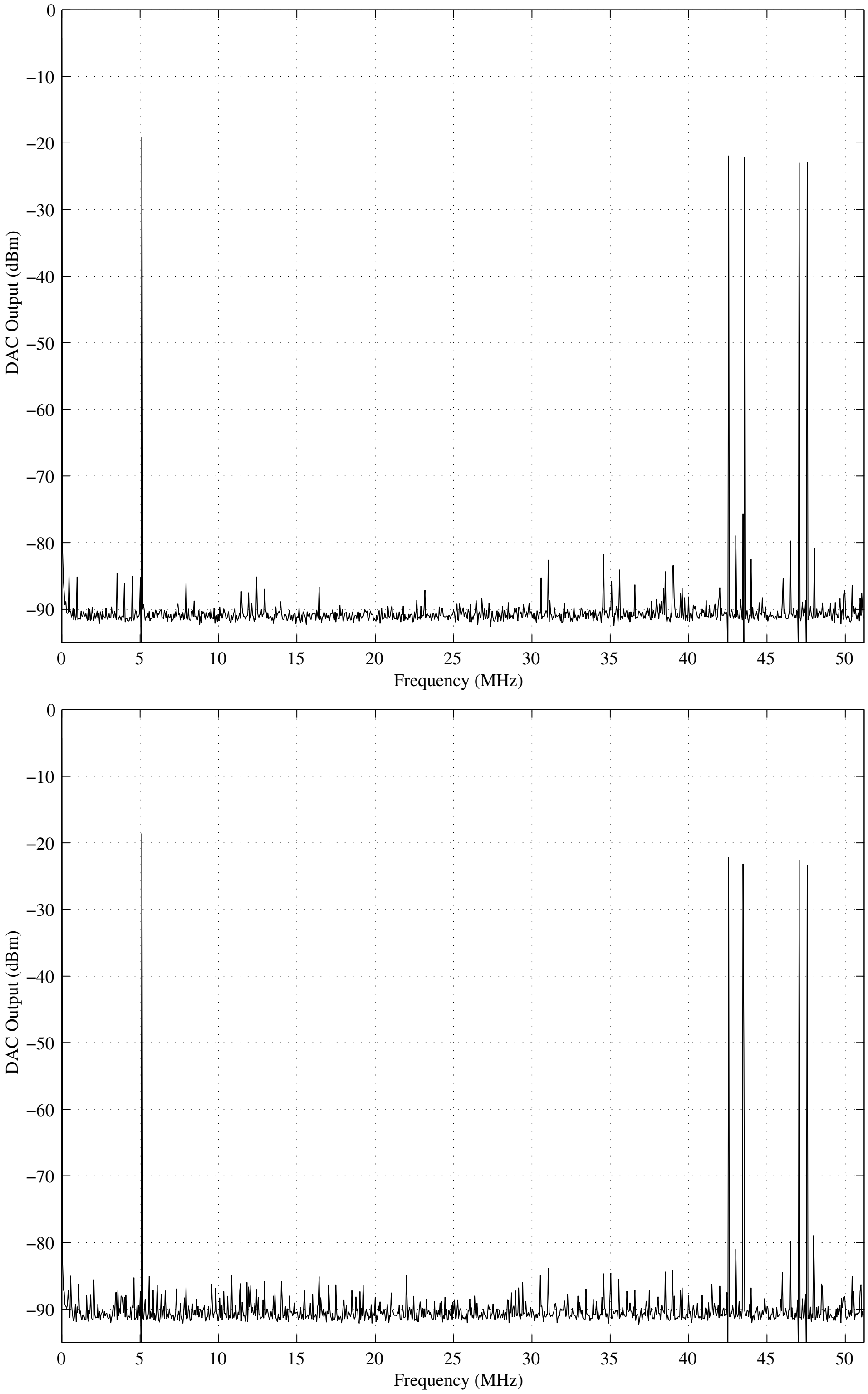

Figure 4.6: Uncompensated(top) and compensated(bottom) spectrum using three two-tone calibration, five-tone test signal at frequencies $f_1 = \frac{407 \cdot f_s}{8192}$, $f_2 = \frac{3399 \cdot f_s}{8192}$, $f_3 = \frac{3479 \cdot f_s}{8192}$, $f_4 = \frac{3759 \cdot f_s}{8192}$, and $f_5 = \frac{3799 \cdot f_s}{8192}$

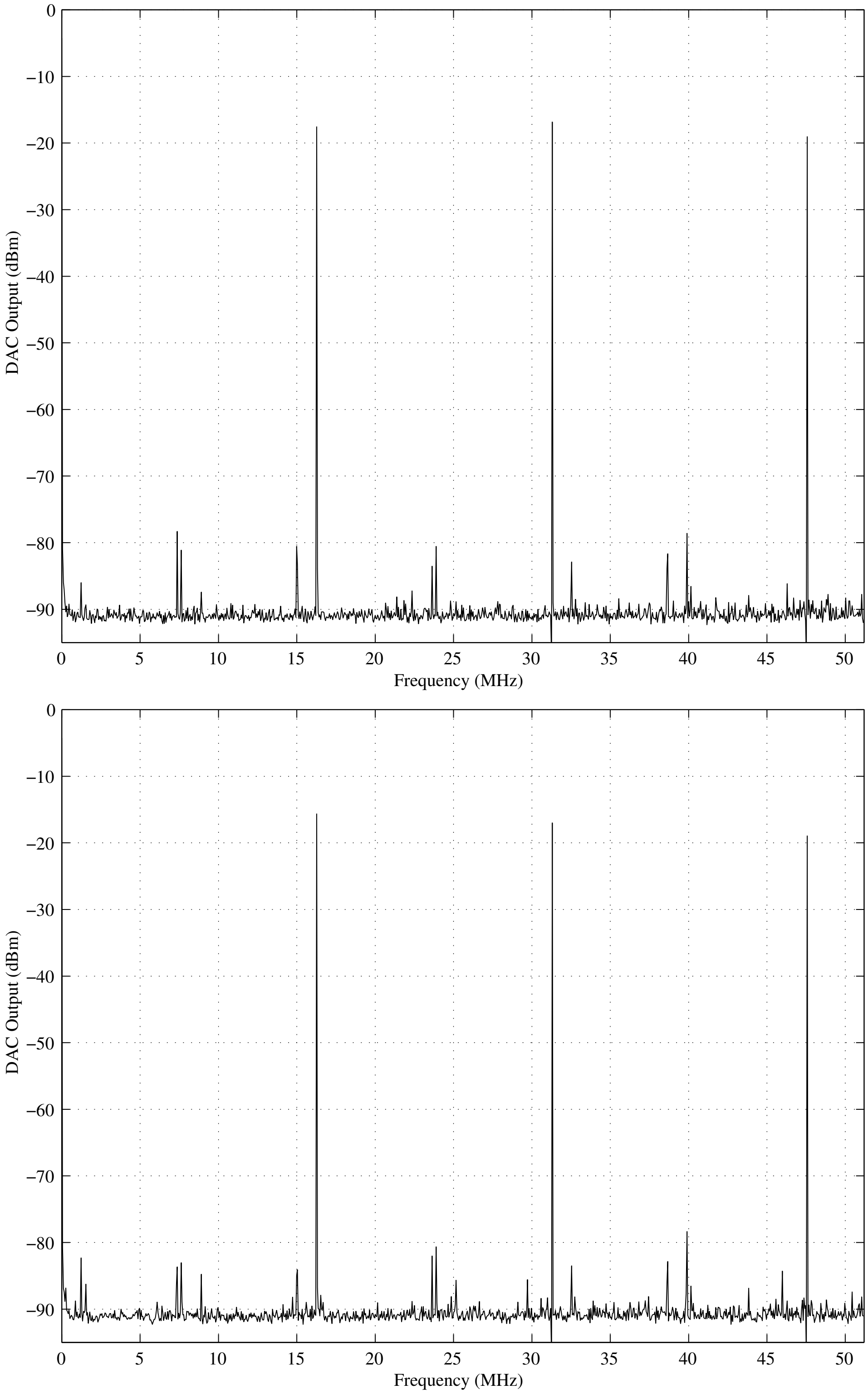

Figure 4.7: Uncompensated(top) and compensated(bottom) spectrum using three two-tone calibration, three-tone test signal at frequencies $f_1 = \frac{1301 \cdot f_s}{8192}$, $f_2 = \frac{2501 \cdot f_s}{8192}$, and $f_3 = \frac{3801 \cdot f_s}{8192}$

rate is 1600 LSBs per oversampled sample. To illustrate slew-limiting, the signal shown in Figure 4.8 has a much lower rate than that actually used in simulation. This slewing rate of 1600 LSBs per sample means that the simulated DAC output can reach full scale in just 3 of 128 oversampled samples.

The new DAC model includes this type of distortion and current/previous sample distortion. The new DAC simulation has 128 times the bandwidth of the original, but measurements on the power spectrum are still made using the previous resolution bandwidth. The calibration routine uses the six-tone calibration waveform and test results are shown in Figures 4.9 through 4.11.

The simulation results provide insight into why the experimental DAC compensation was unsuccessful. This simulation shows that using a current/previous sample model to model the effects of slew-limiting does not work. Another key observation is that the harmonic distortion in the simulation is very similar(in magnitude) to those of the real DAC as shown in Figs. 3.5 through 3.7. This is a good indication that the simulation is modeling the effects of the experimental DAC. The cause of failure would appear to be the use of incorrect basis functions, although it has not yet been shown that the current/previous sample basis function are unimportant. However, this simulation does not indicate the type of basis function that should be used, only that the slew-limiting effect is a likely source of the uncompensatable DAC error.

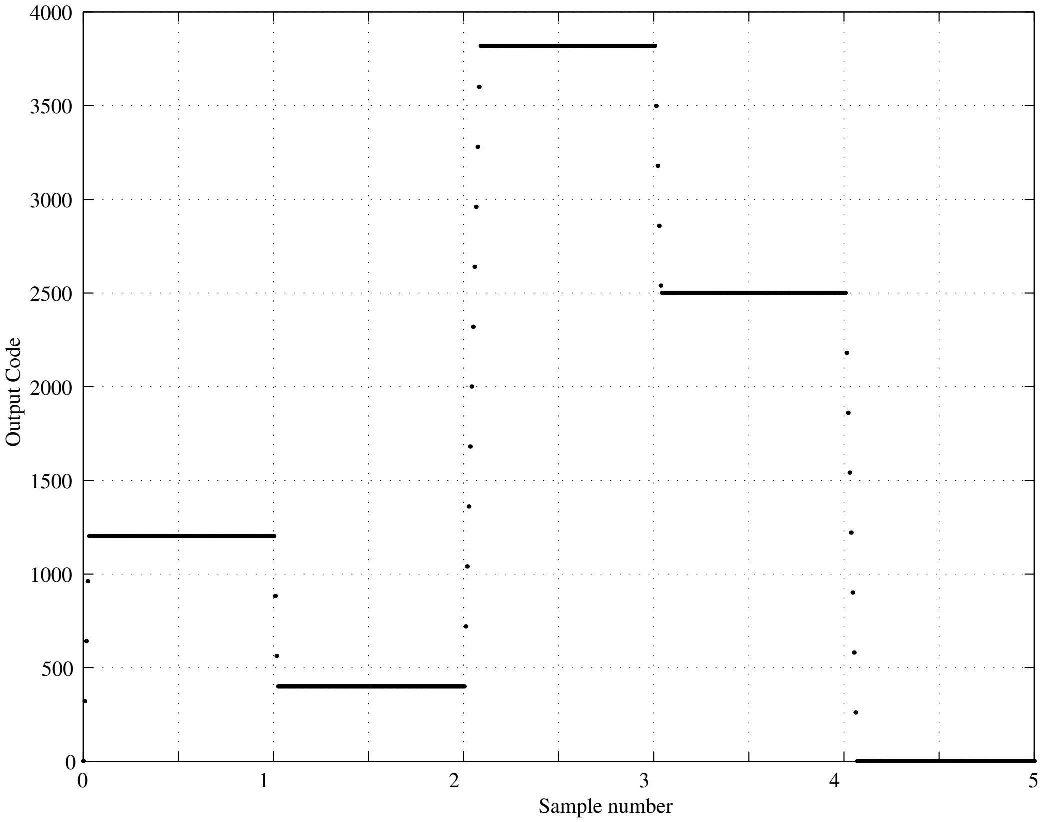

Figure 4.8: Oversampled signal with slew-limiting effect

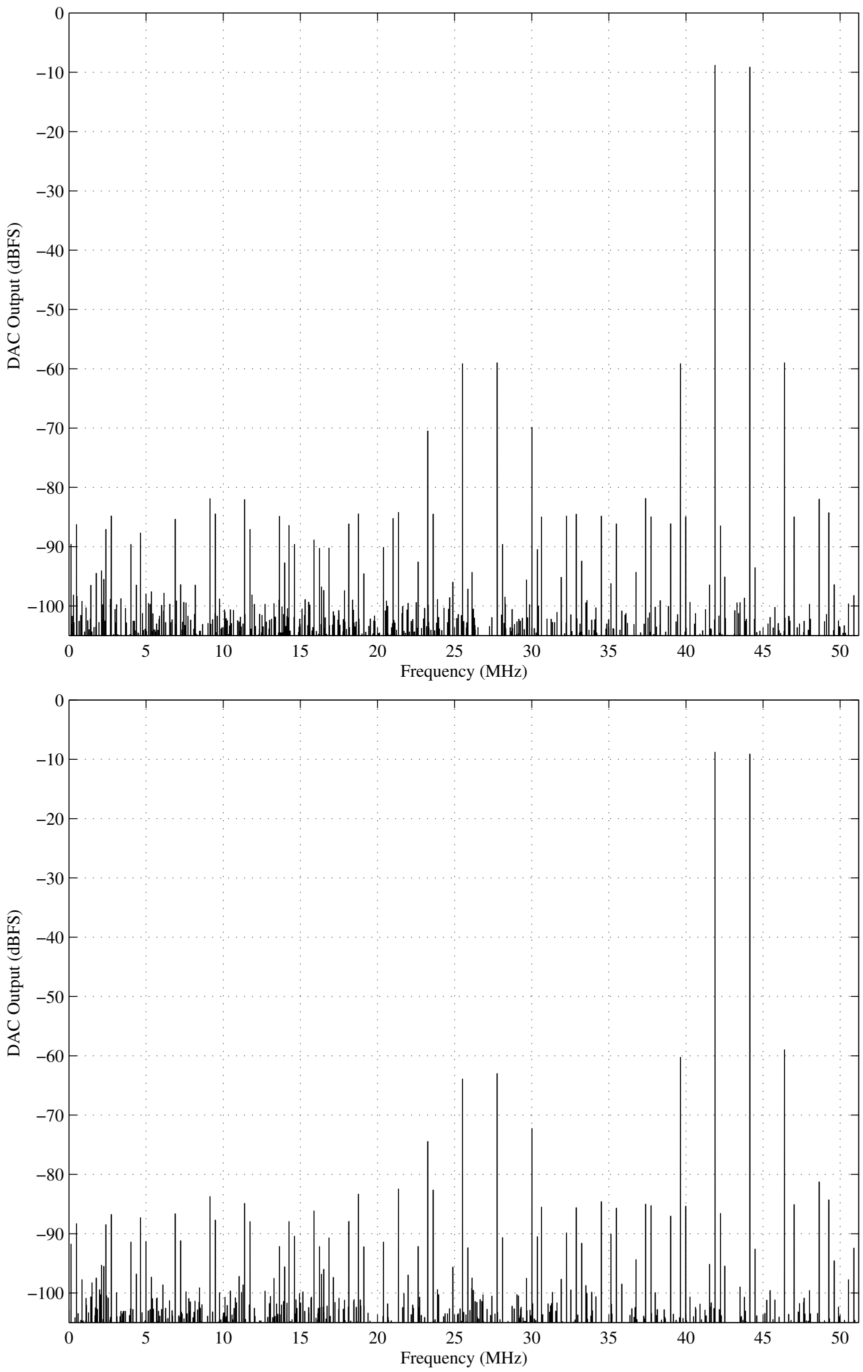

Figure 4.9: Uncompensated(top) and compensated(bottom) simulated spectrum with slew-limiting, test signal at frequencies $f_1 = \frac{3351 \cdot f_s}{8192}$ and $f_2 = \frac{3531 \cdot f_s}{8192}$

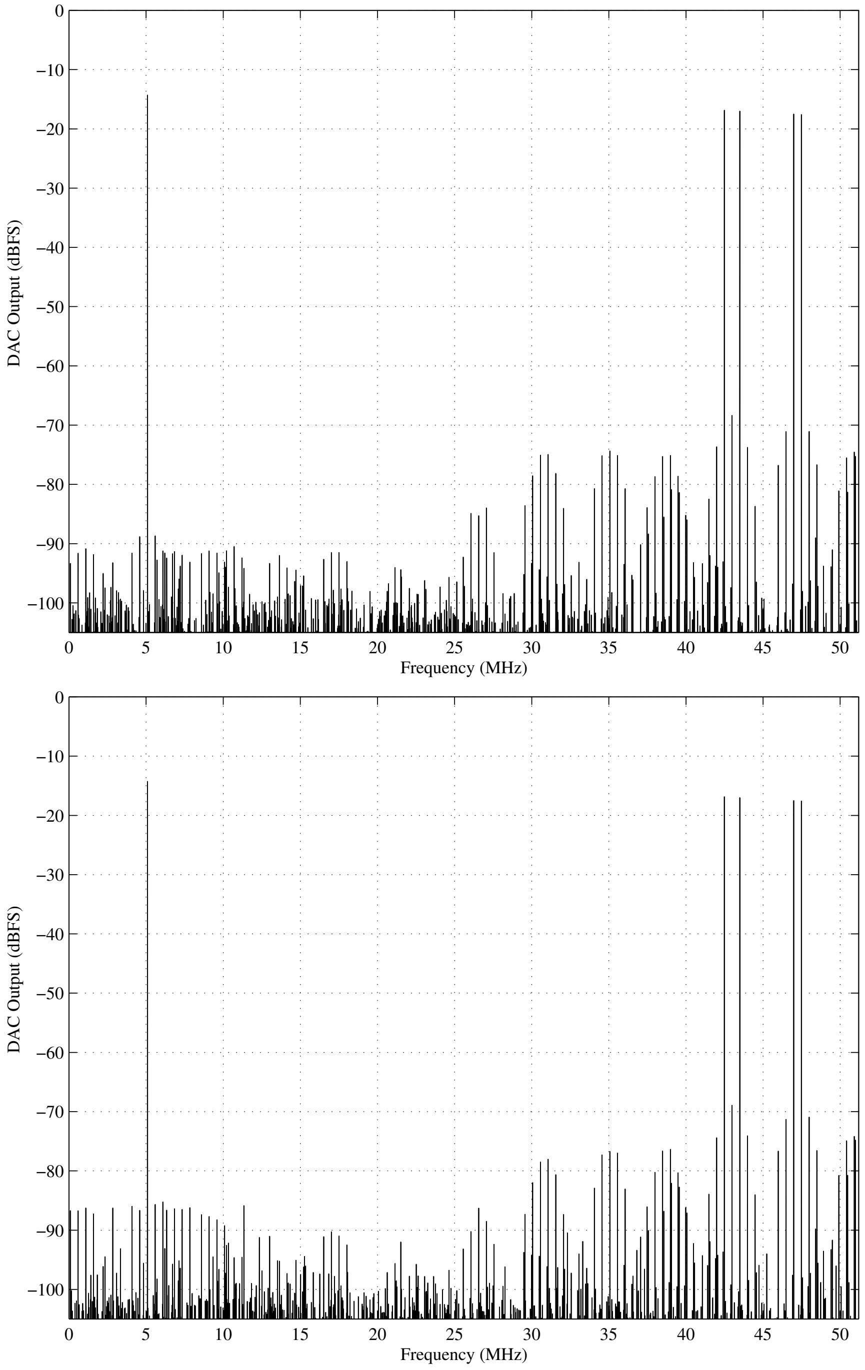

Figure 4.10: Uncompensated(top) and compensated(bottom) simulated spectrum with slew-limiting, five-tone test signal at frequencies $f_1 = \frac{407 \cdot f_s}{8192}$, $f_2 = \frac{3399 \cdot f_s}{8192}$, $f_3 = \frac{3479 \cdot f_s}{8192}$, $f_4 = \frac{3759 \cdot f_s}{8192}$, and $f_5 = \frac{3799 \cdot f_s}{8192}$

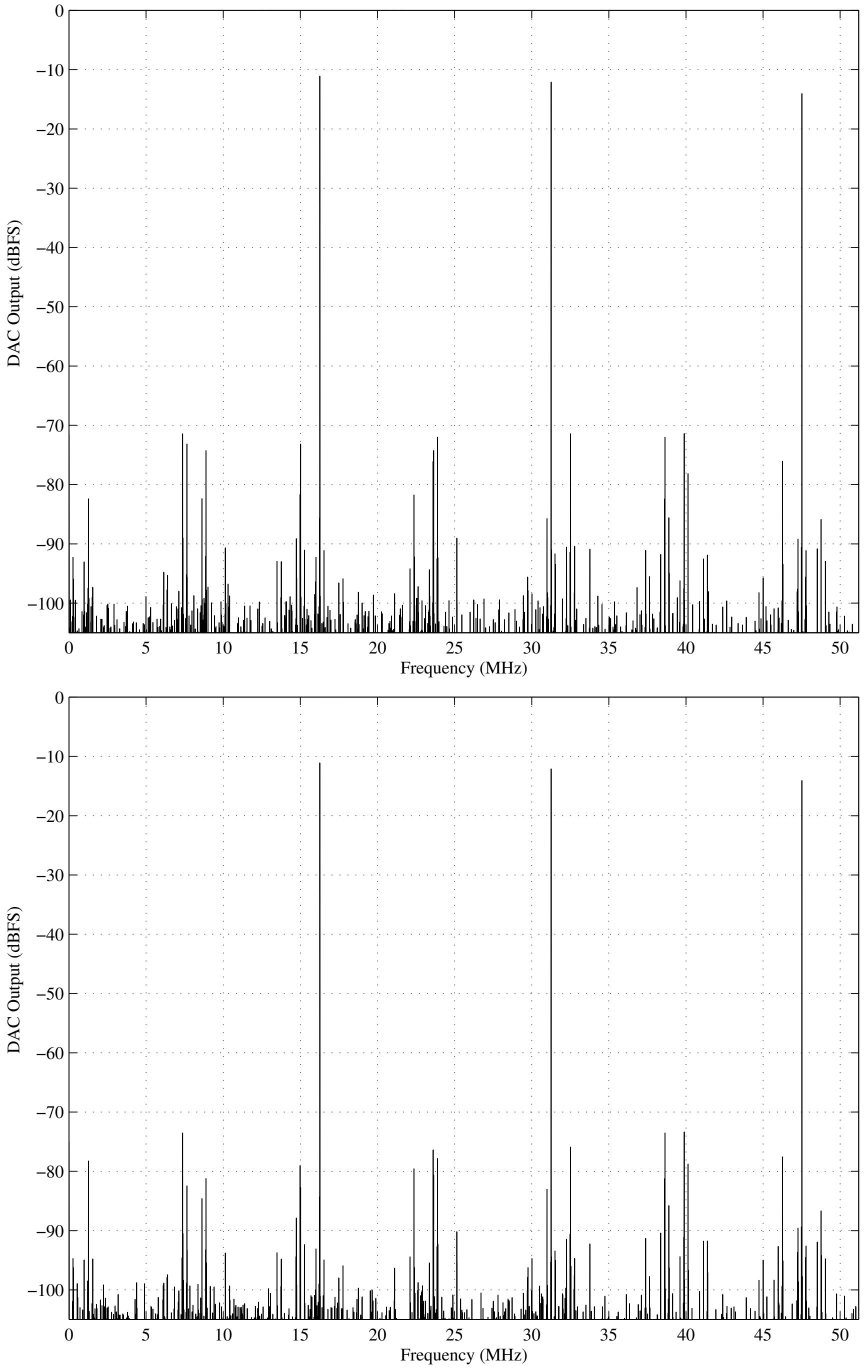

Figure 4.11: Uncompensated(top) and compensated(bottom) simulated spectrum with slew-limiting, three-tone test signal at frequencies $f_1 = \frac{1301 \cdot f_s}{8192}$, $f_2 = \frac{2501 \cdot f_s}{8192}$, and $f_3 = \frac{3801 \cdot f_s}{8192}$

CHAPTER 5

Need for Further Work and Conclusions

5.1 Contributions and Need for Further Work

A method for removing harmonic distortion for a particular waveform was developed and successfully implemented in hardware. Thus desired waveforms can be synthesized using non-ideal DACs. One possible extension of this method would be to shape spectra as desired rather than just removing distortion. If energy can be removed from a particular part of the spectrum, then power can be added up to the limits of the DAC output.

This thesis has provided a calibration method that successfully removed harmonic distortion from a DAC output for an arbitrary signal given that the distortion is dependent on only the current and previous input samples. The general broadband method was not successful when applied to a specific DAC. Insight has been provided into the possible cause of the failure of the calibration. A simulation of slew-limiting demonstrated that if slew-limiting is present in a DAC, then the error model developed in this thesis is not appropriate. The slew-limiting effect would appear to be a dominant cause of the harmonic distortion in DACs, but it is not necessarily only a function of the current and previous sample. Further exploration of the functional relationship of slew-limiting is clearly work that would help to solve the broadband calibration problem.

5.2 Conclusions

This thesis has presented a method for removing harmonic distortion of a DAC for a particular waveform. By making small changes to the input, the distortion can be completely suppressed for a given input sequence. This method provides high SFDR waveforms for any application, especially high precision measurement for adaptive receiver calibration. A general broadband method of calibrating a DAC is also explored. Such a technique would be useful in other applications where there is not a pre-knowledge of the specific desired waveform generating sequence. This calibration technique does not provide results which make much improvement over the original waveform. The failure to remove the distortion suggests that the modeling assumptions were incorrect and one possible source of confusion lies in mechanism of the DAC error. Simulation results are discussed which help to explain why the general waveform calibration failed. In addition to being a function of the current and previous sample, the error appears to have additional error dependence upon other variables which have not yet been determined.

REFERENCES

[1] R. Jacobson. Multiband digital to analog converter compensation. Master's thesis, University of Maine, Dept. of Electrical and Computer Eng., Orono Maine, August 1999.

[2] G. Kelso. Fast calibration of analog to digital converters. Master's thesis, University of Maine, Dept. of Electrical and Computer Eng., Orono Maine, August 1999.

[3] G.M. Kelso, D.M. Hummels, and F.H. Irons. Fast compensation of analog-to-digital converters. In *Proceedings IEEE Instr. and Meas. Tech. Conf.*, Venice, Italy, May 1999.

[4] K. Riley. Dymanic compensation of digital to analog converters. Master's thesis, University of Maine, Dept. of Electrical and Computer Eng., Orono Maine, August 1998.

[5] K.J. Riley, D.M. Hummels, F.H. Irons, and A. Rundell. Dynamic compensation of digital-to-analog converters. In *Proceedings IEEE Instr. and Meas. Tech. Conf.*, Venice, Italy, May 1999.

[6] L.L. Scharf. *Statistical Signal Processing: Detection, Estimation, and Time Series Analysis.* Addison-Wesley, Reading, Massachusetts, 1991.

BIOGRAPHY OF AUTHOR

Greg Friel was born in North Tonawanda, New York on March 11, 1976. He received his high school education from Jay High School in Jay, Maine in 1994. He entered the University of Maine in 1994 and obtained his Bachelor of Science degree in Electrical Engineering in 1998. In May 1998, he was enrolled for graduate study in Electrical Engineering at the University of Maine where he served as a Research Assistant. Current research interests include communications, system modeling and signal processing. He plans to continue his education at Purdue University where he has entered a Ph.D. program. He is a candidate for the Master of Science degree in Electrical Engineering from the University of Maine in May, 2000.